

Hyperscaling violation : a unified frame for effective holographic theories

Bom Soo Kim

Raymond and Beverly Sackler School of Physics and Astronomy,
Tel Aviv University, 69978 Tel Aviv, Israel
bskim@post.tau.ac.il

Abstract

We investigate systematic classifications of low energy and lower dimensional effective holographic theories with Lifshitz and Schrödinger scaling symmetries only using metrics in terms of hyperscaling violation (θ) and dynamical (z) exponents. Their consistent parameter spaces are constrained by null energy and positive specific heat conditions, whose validity is explicitly checked against a previously known result. From dimensional reductions of many microscopic string solutions, we observe the classifications are tied with the number of scales in the original microscopic theories. Conformal theories do not generate a nontrivial θ for a simple sphere reduction. Theories with Lifshitz scaling with one scale are completely fixed by θ and z , and have a universal emblackening factor at finite temperature. Dimensional reduction of intersecting M2-M5 requires, we call, spatial anisotropic exponents (\sharp), along with $z = 1, \theta = 0$, because of another scale. Theories with Schrödinger scaling show similar simple classifications at zero temperature, while require more care due to an additional parameter being a thermodynamic variable at finite temperature.

Contents

| | | |
|----------|---|-----------|
| 1 | Introduction : hyperscaling violation and effective theories | 2 |
| 2 | Theories with Lifshitz scaling | 8 |
| 2.1 | Review and constraint plots | 9 |
| 2.2 | Entanglement entropy to thermal entropy | 10 |
| 2.3 | An explicit solution : EMD theories | 12 |
| 2.3.1 | Thermodynamics | 16 |
| 2.3.2 | Constraints on the parameter space | 17 |
| 2.4 | $d + 2$ dimensional EMD solutions | 18 |
| 3 | Theories with Schrödinger scaling I | 19 |
| 3.1 | String theory realizations of Schrödinger backgrounds | 21 |
| 3.1.1 | Determination of the dynamical exponent | 22 |
| 3.1.2 | Thermodynamic Properties | 24 |
| 3.1.3 | Reduction to Lifshitz type theories | 24 |
| 3.2 | Entanglement entropy | 25 |
| 3.3 | Searching for effective theories | 28 |
| 4 | Theories with Schrödinger scaling II | 29 |
| 4.1 | String theory realizations for ALCF | 30 |
| 4.1.1 | Thermodynamic Properties | 32 |
| 4.1.2 | Reduction to theories with Lifshitz scaling | 33 |
| 4.2 | Entanglement entropy | 33 |
| 4.3 | Searching for ALCF effective theories | 35 |
| 5 | Summary and Outlook | 36 |
| A | Dimensional reduction of theories with Lifshitz scaling | 39 |
| A.1 | Near extremal Black Dp branes | 39 |
| A.2 | Black M2 brane | 41 |
| A.3 | Black M5 brane | 42 |
| A.4 | Dp-D(p+4) branes | 43 |
| A.5 | Intersecting and interpolating M-branes | 45 |

| | | |
|----------|--|-----------|
| B | Dimensional reduction of solutions with Schrödinger scaling | 46 |
| B.1 | ‘Conformal’ cases | 47 |
| B.2 | NS5A brane | 48 |
| B.3 | NS5B brane | 51 |
| B.4 | F1 brane | 51 |
| B.5 | KK monopole | 52 |

1 Introduction : hyperscaling violation and effective theories

The concept of hyperscaling violation [1], developed in condensed matter [2][3], has attracted much attention recently [4]-[35] in the context of gauge gravity duality [36][37]. For example, hyperscaling violation provides a useful way to realize “compressible matters” in $(2 + 1)$ dimensions [1][38][39] and to pursue the holographic realization of systems with Fermi surfaces [6][7]. (See earlier efforts on considering holographic Fermi surfaces *e.g.* in [40]-[43].) Many physically interesting materials at zero temperature, such as high T_c cuprates superconductors, heavy fermion superconductors and organic insulators, are compressible, meaning that the “density” of their ground states can be dialed by some quantum tuning parameters, such as chemical doping, pressure and chemical potentials, respectively. As explained nicely in [1], the ground states of compressible quantum matters can be described by a modified Hamiltonian $\mathcal{H}' = \mathcal{H} - \mu\mathcal{Q}$ in the presence of an $U(1)$ symmetry, where μ and \mathcal{Q} are chemical potential and charge associated with the $U(1)$ symmetry, which commutes with the original Hamiltonian \mathcal{H} . The system needs gapless excitations and requires to satisfy $d\langle\mathcal{Q}\rangle/d\mu \neq 0$ at $T = 0$. Using scaling arguments, one can get $d\langle\mathcal{Q}\rangle/d\mu \sim T^{d-1}$, where d is the number of spatial dimensions. Thus one naturally has compressible matters for $d = 1$ (Luttinger liquids), while it is difficult to realize them for $d \neq 1$. This difficulty can be overcome in the presence of hyperscaling violation, which effectively gives $d_{\text{eff}} = d - \theta$. Thus the compressible matter at zero temperature in $2 + 1$ dimensions can be achieved with $\theta = 1$ [1].

Hyperscaling violation is realized in holography as a property of the metric, as was first pointed out in [5], based on the extremal solutions at finite density that were found in [4]. Its implications and importance for strongly coupled condensed matter systems were developed further in [7]. It has been argued that holographic backgrounds with dual Fermi surfaces can be consistently obtained in the systems satisfying $\theta = d - 1$, and thus $\theta = 1$ for $d = 2$, based on various physical grounds [6][7].¹ In particular, this particular system shows a logarithmic violation of the area law in the holographic entanglement entropy calculation,

¹ This is well fitted with the field theoretic picture outlined in the previous paragraph. See [44] for an example of compressible matter with the Fermi surfaces present for different doping.

which is adapted as a working definition of holographic systems with Fermi surfaces [6] based on field theoretic results [45]. The holographic entanglement entropy [46]-[49] is further used to identify some novel phases, which interpolates between the logarithmic violation and extensive volume dependence of entanglement entropy [8][11].

Our aim

While the notion of hyperscaling violation is developed in condensed matter community, it can also serve as a useful tool for high energy community as well. Here we would like to consider several different classes of microscopic string theory solutions and their simplest dimensional reductions along the compact coordinates. It becomes clear that hyperscaling violation effects are prevalent upon dimensionally reducing the microscopic string solutions. One simple observation is that θ captures the degree of the violation of the conformal / scaling symmetry of the original solutions as well as the degree of compactification. For example, conformally invariant systems such as D3, M2, M5, D1-D5 and their non-relativistic versions generated by the null Melvin twist show $\theta = 0$ upon simple sphere reductions. Motivated by these observations and earlier efforts [8][11], we investigate the following program.

- A. The hyperscaling violation exponent θ can serve as a unified framework for classifying the lower dimensional and low energy effective *holographic* theories with scaling symmetries, especially the Lifshitz and Schrödinger scaling.
- B. We only consider gravitational metrics for the classifications with undetermined exponents (z, θ) , without referring to the full solution, such as action and matter contents.²
- C. We constrain the parameter space of the consistent solutions using the null energy condition, entanglement entropy analysis and the thermodynamic stability, especially the positivity of the specific heat, along the line of [6][8][11].

This program for constraining the parameter space of the theories with Lifshitz scaling at finite temperature is explicitly compared against the known efforts to do so with full solution in the context of the Einstein-Maxwell-Dilaton theories with two parameters [4][51][52]. These two results are in very good agreements. Even though constraining the consistent parameter spaces using the null energy conditions and positivity of specific heat constraint is expected to serve as a rough guide, our detailed and explicit comparison provides us enough

² One metric can be supported by more than one set of matter sources and action, see *e.g.* [50]. Thus classifying effective theories with full solutions would be redundant for investigating the low energy universal properties, which are independent of details, not to mention the physical quantities directly related to metric.

confidences for the validity to do so.³

Outline and Main points

We consider the following general metric to classify lower dimensional and low energy effective theories, holographically dual to field theories with Lifshitz and Schrödinger scaling symmetries in d spatial dimensions at zero temperature

$$ds^2 = r^{-2+2\theta/D} \left(-b r^{-2(z-1)} dt^2 - 2a dt d\xi + dr^2 + \sum_{i=1}^c dx_i^2 + \sum_{j=c+1}^d \eta_j(r, t, \vec{x}) dx_j^2 \right), \quad (1.1)$$

where θ and z are the hyperscaling violation and dynamical exponents, respectively.⁴ Note that we split the d spatial coordinates into two. The first c dimensions have been put into a standard form, dx_i^2 , using coordinate transformations.⁵ We call these coordinates as *reference* coordinates. While $\eta_j(r, t, \vec{x})$ can take any general form to provide various different scaling properties for each particular spatial direction, here we consider the simplest cases : the parameter η has only the radial dependence as

$$\eta_k(r, t, \vec{x}) \equiv r^{2-2\sharp_{k|1}}, \quad (1.3)$$

where $\sharp_{k|1}$ denotes “spatial anisotropic exponent” of the k^{th} coordinate relative to the reference coordinate x_1 . These spatial anisotropic exponents are naturally realized in the intersecting Dp-Dq brane systems §A.4 and M-brane systems §A.5. We expect that there are more general class of systems with the spatial anisotropy.

³Can we say something about the landscape of the string theory vacua and the corresponding classification? While classifying them only with metrics would be much simpler, the answer is far from clear, and we have nothing to say about it. Our program might be more relevant for classifying general throat geometries with more exponents. We are grateful to Piljin Yi for the discussions and comments.

⁴It is clear that the boundary sits at $r \rightarrow 0$ from the context. One can use different, yet equivalent, coordinate system using $r = \frac{1}{u}$ (now the boundary sits at $u \rightarrow \infty$) as

$$ds^2 = u^{2-2\theta/D} \left(-bu^{2(z-1)} dt^2 - 2adt d\xi + \frac{du^2}{u^4} + \sum_{i=1}^c dx_i^2 + \sum_{j=c+1}^d \eta_j(u, t, \vec{x}) dx_j^2 \right), \quad (1.2)$$

which provides the identical exponents θ, z and \sharp . This distinction of the correct coordinate system is important to identify these exponents uniquely. Still the distinction can be unclear because the metric at hand is valid only for a given range of the radial coordinate. Moreover, this distinction can be ambiguous at its fundamental level. One particular example is non-commutative super Yang-Mills due to the UV-IR correspondence [53]-[56]. Similar features are expected for dipole field theories [57][58] and puff field theories [59][60]. We are grateful to Ori Ganor and Sanny Itzhaki for their comments and discussions on them.

⁵ There are some exceptional cases for the Schrödinger type solutions to do this successfully. Schrödinger symmetry require the combination $-2dt d\xi + dr^2$, which does not allow further coordinate redefinitions on the radial coordinate. One explicit example is considered in detail in §B.1 and §B.3.

The metric is invariant under the following scaling transformations :

$$t \rightarrow \lambda^z t, \quad \xi \rightarrow \lambda^{2-z} \xi, \quad r \rightarrow \lambda r, \quad (1.4)$$

$$x_i \rightarrow \lambda x_i, \quad i = 1, \dots, c, \quad (1.5)$$

$$x_j \rightarrow \lambda^{\sharp_{j|i}} x_j, \quad j = c+1, \dots, d. \quad (1.6)$$

It is clear that $z = 1$ and $\sharp = 1$ represent the usual scaling transformation of the relativistic Poincaré invariant systems. Thus $\sharp \neq 1$ signifies the spatial anisotropy and broken rotational symmetries between the reference coordinates and the anisotropic coordinates.

It turns out that there can be several equivalent sets of the exponent for the cases with the nontrivial spatial anisotropic exponents, due to the fact that any spatial coordinate is qualified to take the role of the reference coordinate. To illustrate this point, let us change the reference coordinate from x_1 to x_d for a simple case $a = 0, b = 1$. Then we get

$$r^{2\theta/D-2\sharp_{d|1}} \left(-r^{2\sharp_{d|1}-2z} dt^2 + r^{2\sharp_{d|1}-2} dr^2 + r^{2\sharp_{d|1}-2} dx_1^2 + \dots + dx_d^2 \right), \quad (1.7)$$

which gives the following new exponents

$$\theta' = \frac{\theta}{\sharp_{d|1}}, \quad z' = \frac{z}{\sharp_{d|1}}, \quad \sharp'_{1|d} = \frac{1}{\sharp_{d|1}}, \quad \dots, \quad (1.8)$$

after redefining the radial coordinates $r \rightarrow r^{\frac{1}{\sharp_{d|1}}}$. The physical properties described by this set of exponents are equivalent to those described by θ, z and the original spatial anisotropic exponents $\sharp_{i|1}, i = 2, \dots, d$. If the original anisotropic exponent $\sharp_{d|1}$ is negative, it is required to use the coordinate system described in footnote 4 and the results are the same. The case $\sharp_{d|1} = 0$ requires a non-polynomial transformation to achieve the goal, and eventually one sees that the resulting exponents are not well defined. It is plausible that this case can be formulated with the ration θ'/z' fixed, while $\theta' \rightarrow \infty$ and $z' \rightarrow \infty$ [13].

With these general properties, we consider the physically interesting theories with different scaling properties in turn, depending on the parameters D, a, b, θ, z and η_i . We also organize our paper accordingly.

- I. Relativistic solutions with full Lorentz symmetry. This case has the parameters $D = d, b = 1, a = 0, z = 1$ and $\eta_k = 1, k = c+1, \dots, d$, which has the full rotational symmetry on the d spatial directions. This geometry includes the well known AdS spaces with conformal symmetry for $\theta = 0$, which is valid for all the energy scales. $\theta = 0$ represents the fact that there exists no non-trivial energy scale in the original microscopic string solution. Examples include the dimensional reductions of the D3, M2 and M5 solutions, which are considered in §A.1 A.2 and A.3, respectively.

The near extremal black Dp brane solutions are another examples of this type, but now with non-zero hyperscaling violation exponent θ . It is straightforward to see that non-zero hyperscaling violation is directly related to the fact that there is a non-trivial dimensionful parameter in the original Dp brane metrics, which is explicitly demonstrated with dimensional reductions in §A.1.

The theories with $z = 1$ are the special cases of the Lifshitz backgrounds. Thus we consider the relativistic cases with $z = 1$ as part of the following item [II].

- II. Lifshitz type solutions with non-zero θ and general z . The parameters are $D = d, b = 1, a = 0$ and $\eta_k = 1, k = c + 1, \dots, d$. The physical aspects of the Lifshitz theories with general scaling symmetry z and the hyperscaling violation exponent θ are already considered in [8]. It is further considered below in §2.1 and in §2.2. Especially we depicted allowed regions (figure 1) based on the program explained in *our aim*.

This type of gravity solutions are constructed for the low energy description of Einstein-Maxwell-Dilaton system [4] and shown to be the most general IR asymptotic solutions with one gauge and one scalar fields[5]. It is embedded in higher dimensional theories[5]. Its finite temperature generalizations are proposed and analyzed in [4]. This system is explicitly considered in §2.3 for $d = 2$ and in §2.4 for arbitrary d , where we re-express the full system in terms of the parameters (z, θ) along with the thermodynamic properties. In the figure 2 in §2.3.2, we also present allowed regions of the parameter space of (z, θ) from different set of consistency conditions using the full solution [4][51][52]. We compare these two different allowed regions and found good agreements.

We would like to mention that all the worked-out examples of string theory motivated solutions along with the examples [4] have a particular form of the emblackening factor

$$f(r) = 1 - \left(\frac{r}{r_H} \right)^{d+z-\theta}, \quad (1.9)$$

which reflects the scaling properties and is very interesting.

- III. Intersecting Dp-Dq and M brane systems with $a = 0$ and $b = 1$. The nontrivial spatial anisotropic exponents, $\eta_k \neq 1$, naturally emerge in these systems.⁶ In Dp-D(p+4), ($p = 0, 1, 2$), systems, we get the exponents

$$d = p + 4, \quad \theta = \frac{1 - p^2}{2 - p}, \quad z = 1, \quad \sharp_{p+4|p} = \frac{1 - p}{2(2 - p)}. \quad (1.10)$$

⁶We are grateful to Yaron Oz and Cobi Sonnenschein for valuable comments on Dp-D(p+4) brane systems and associated anisotropic exponents. $p = 0$ and $p = 2$ cases actually do not generate non-trivial \sharp . $p = 1$ case can be further compactified down to $p + 2$ dimensional metric for the compact $M_4 = T^4$ or K_3 . Intersecting M2-M5 branes with non-compact directions is presented in §A.5.

Let us consider D1-D5 system, which is known to have $AdS_3 \times M_4$, namely AdS_3 conformal factor in the dimensionally reduced metric. Correspondingly, we get $\theta = 0$. The effective metric is

$$ds_{D1D5}^2 = \sqrt{Q_1 Q_5} u^2 \left[-f dt^2 + dx_1^2 + \frac{1}{u^4} \frac{du^2}{f} + \frac{Q_1}{u^2} ds_{M_4}^2 \right], \quad (1.11)$$

which shows the non-trivial spatial anisotropy, stemming from the relative scale between these two spaces AdS_3 and M_4 . This is described in §A.4 in detail. Intersecting and interpolating M-branes are also considered in §A.5 to show similar features. Recently, the hyperscaling violation exponent in the intersecting brane systems are considered in [14][16][23][28].

IV. Schrödinger metrics with general θ and z . The parameters are $D = d + 1$, $a = 1$ and $\eta_k = 1, k = c + 1, \dots, d$. The physical aspects with hyperscaling violation at zero temperature are discussed in [11]. Surprisingly, we find a candidate Schrödinger background that possesses dual Fermi surfaces according to [6][7] from a simple dimensional reduction of non-relativistic NS5A brane in §B.2. The background reveals the relation $\theta = d + 1 - z$, which is worked out in [11] based on “codimension 2” minimal surface prescription. We further investigate other physical properties of this non-relativistic NS5A brane in §B.2. Lifshitz background with dual Fermi surfaces has been also claimed in [10]. (See also [17][30] for the discussions of the hyperscaling violation on Schrödinger space.)

Finite temperature generalizations from effective low energy and lower dimensional point of view turn out to be more difficult than expected, due to the non-trivial asymptotic form and an additional dimensionful parameter b generated by the null Melvin twist. This parameter b serves as an independent thermodynamic variable, along with r_H , and thus can not be ignored. Constructing general low energy effective metrics based on symmetries is a highly non-trivial task. Thus we consider non-relativistic Dp branes generated by the null Melvin twist investigate their physical properties at finite temperature and perform the dimensional reductions of them in §3.1. Along the way, we identify the exponents θ and z in §3.1.1, which turns out to be not straightforward. In §3.2, entanglement entropy at finite temperature is considered to show that it reproduce the thermal entropy at high temperature limit and zero temperature entanglement entropy at low temperature limit.

Finally, we consider a class of effective Schrödinger backgrounds at finite temperature in §3.3. We present a plot for the allowed regions in the figure 3 for $z > 0$ by using the null energy, entanglement entropy conditions and specific heat constraint for fixed chemical potential associated with the null coordinate ξ .

There exist two different geometric realizations with Schrödinger symmetry in holographic approach, Schrödinger backgrounds with $b = 1$, described in §3, and AdS in light-cone frame (ALCF) with $b = 0$. §4 contains the parallel investigations of ALCF compared to the Schrödinger background §3. In particular, the dynamical exponent z remains unfixed even after the dimensional reduction, which is one of the reasons we separate our discussions for these two geometric realizations of Schrödinger holography. Schrödinger background and ALCF have the same thermodynamic properties. By rewriting their metrics in a more organized form as equations (3.7) and (4.8), we find an important technical detail responsible for the fact. Basically, the newly introduced K factor from the null Melvin twist in (3.7) does not enter the thermodynamic analysis.

The basic properties and the dimensional reductions of several different systems are investigated in detail in appendix §A and §B. Even though these examples are far from the exhaustive lists of the low energy and lower dimensional holographic theories, we hope they serve to show the hyperscaling violation exponent θ provides a unified framework for the low energy and lower dimensional holographic theories.

2 Theories with Lifshitz scaling

Theories with the Lifshitz scaling symmetries [61][62] with dynamical exponent z and hyperscaling violation exponent θ have been considered in [8] from the metric point of view without referring to matter contents. The full extremal solutions were constructed and analyzed in [4]. Their scaling properties, including their violation of hyperscaling was pointed out later in [5][7]. The explicit solution is developed in the context of the holographic bulk solutions with the Einstein-Maxwell action with a Dilaton (EMD theories) [63]-[74].

In this section, we first review some salient features of the known results in §2.1, along with the analysis of the entanglement entropy at finite temperature to thermal entropy in §2.2. From our program to classify the low energy and lower dimensional effective holographic theories, we would like to check whether the consistency conditions we impose are reasonable guides. For this purpose, we make plots of the consistent regions of the parameter spaces (z, θ) for 2 and 3 spatial dimensions using the null energy condition and positive specific heat constraint. We call the allowed regions (I) from these constraints.

Then we consider the explicit solution [4][51][52][71] with two parameters (γ, δ) and map it in terms of the parameters (z, θ) for $d = 2$ in §2.3 and for general dimensions in §2.4. For the future references, we list also the thermodynamic properties in term of the parameters (z, θ) in §2.3.1. The allowed regions of the parameter spaces (γ, δ) at zero temperature are explicitly analyzed by various conditions, such as Gubser's criteria [75] and well defined

fluctuation problems in [4][51][52][71]. In §2.3.2, we plot the allowed regions (II) in terms of (z, θ) including the positive specific heat constraint at finite temperature. These two allowed regions (I) and (II), upon including the positive specific heat constraint, are identical, which provides a positive sign for the program to constrain the allowed regions from the low energy and lower dimensional point of view.

2.1 Review and constraint plots

The metric we are interested in is described by

$$ds_{d+2}^2 = r^{-2(d-\theta)/d} \left(-r^{-2(z-1)} f(r) dt^2 + \frac{dr^2}{f(r)} + \sum_{i=1}^d dx_i^2 \right),$$

$$f(r) = 1 - \left(\frac{r}{r_H} \right)^{d+z-\theta}. \quad (2.1)$$

Physical properties of this metric emphasizing the role of the hyperscaling violation exponent θ are analyzed in detail in [8].

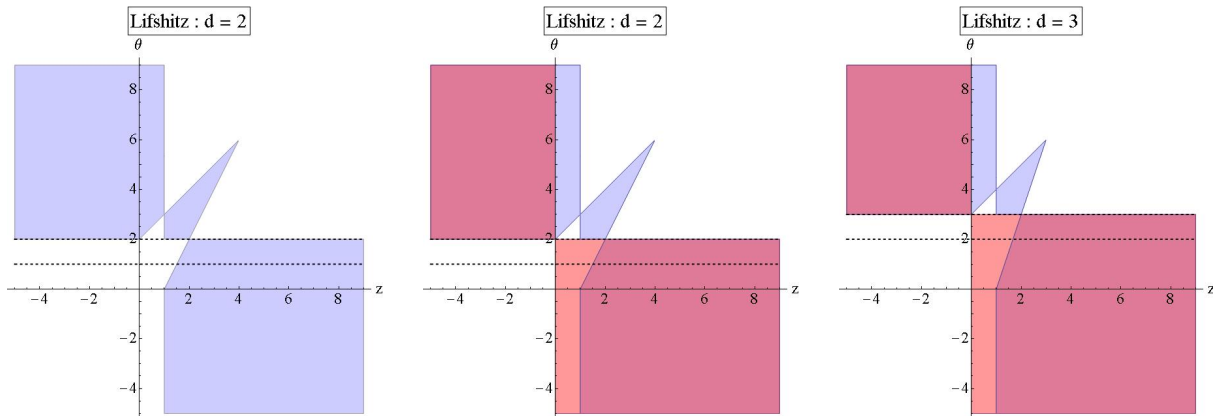


Figure 1: The left plot shows the allowed regions for the Lifshitz geometry based on the null energy conditions, along with the region between two dashed lines indicating some novel phases from the entanglement entropy analysis [8]. The middle plot shows the allowed (dark purple) regions after taking into account of the specific heat condition (2.3). The right plot ($d = 3$) shows the regions allowed by the null energy condition (blue) and the specific heat (red), and thus the dark purple regions, allowed regions (I), are allowed by both conditions. These conditions indicate that physically sensible theories are required to $\theta \geq d$ for $z \leq 0$, while they are required to have $\theta \leq d$ for positive z . It is further suggested that the region $\theta \geq d$ and $z \leq 0$ are unstable from the entanglement entropy analysis [8]. Thus only the bottom right region is allowed and covers $z \geq 1$ and also $\theta \leq d$, except small top left corner of that region.

Without referring to specific matter contents to support the background, the authors of [8] restrict the consistent parameter spaces with null energy conditions at zero temperature

following [6][7]. See also the usage of null energy condition [76]. The condition is given by

$$(d - \theta)(d(z - 1) - \theta) \geq 0, \quad (z - 1)(d + z - \theta) \geq 0, \quad (2.2)$$

which is depicted in the left plot of figure 1 for $d = 2$ case. The allowed regions are further constrained by some thermodynamic stability, mainly the positivity of the specific heat at finite temperature, which is

$$\frac{d - \theta}{z} \geq 0. \quad (2.3)$$

The result is summarized in the middle plot of figure 1. These constraints are not expected to be completely accurate, but it seems to serve as a good guide for all the dimensionally reduced microscopic string solutions considered in the appendix §A.

Note the specific form of the emblackening factor $f(r)$. The r dependent power is *a priori* not fixed by any symmetry or dimensional analysis, especially from the view of the resulting effective theories which are dimensionally reduced from string theory solutions. Yet, this particular combination $f(r) = 1 - (r/r_H)^{d+z-\theta}$ is valid for the dimensional reduction of the black Dp brane [8], black M2 and M5 branes, as well as a large class of exact black hole solutions [4][71]. Some of them are further studied in the appendix §A. Interestingly, the theories with Schrödinger isometries, upon dimensionally reduced along the null direction ξ , also exhibit this property as explicitly shown in §3.1.3 and §4.1.2. This combination $d+z-\theta$ is tied with the physical property of the thermal entropy S_T in terms of the temperature T

$$S_T \sim T^{(d-\theta)/z}, \quad (2.4)$$

which can be easily verified from $T \sim r_H^{-z}$ and $S_T \sim r_H^{\theta-d}$. It will be interesting to check whether these properties are true for all the lower dimensional Lifshitz type solutions, which have their microscopic string solutions.

2.2 Entanglement entropy to thermal entropy

Entanglement entropy has been a useful tool for classifying the phases of the matter [45], and it has been actively discussed in holographic context, see *e.g.* [46]-[49]. The cross-over from the entanglement entropy to thermal entropy in Lifshitz space is already studied in [8] motivated by [77]. Here we review the result for the comparison to the Schrödinger geometry we study in detail in the following sections.

The entanglement entropy of the metric (2.1) with finite temperature can be computed for a strip

$$-l \leq x_1 \leq l, \quad 0 \leq x_i \leq L, \quad i = 2, \dots, d \quad (2.5)$$

in the limit $l \ll L$. The strip is located at $r = \epsilon$, and the profile of the surface in the bulk is given by $r = r(x_1)$. The minimal surface has a turning point at $r = r_t$. Thus, to get the entanglement entropy, we can evaluate the following expressions

$$l = \int_0^{r_t} dr \frac{1}{\sqrt{f}} \frac{(r/r_t)^{\alpha_2}}{\sqrt{1 - (r/r_t)^{2\alpha_2}}}, \quad \mathcal{A} = L^{d-1} \int_\epsilon^{r_t} dr \frac{1}{\sqrt{f}} \frac{r^{-\alpha_2}}{\sqrt{1 - (r/r_t)^{2\alpha_2}}}, \quad (2.6)$$

where $\alpha_2 = d - \theta$.

Assuming $\alpha_2 > 0$, we can rewrite the integrals as

$$l = r_t \int_0^1 d\omega \frac{\omega^{\alpha_2}}{\sqrt{1 - (\gamma\omega)^{\alpha_2+z}} \sqrt{1 - \omega^{2\alpha_2}}}, \quad (2.7)$$

and, following [77]

$$\mathcal{A} = L^{d-1} r_t^{1-\alpha_2} \int_{\epsilon/r_t}^1 d\omega \left(\left[\frac{\omega^{-\alpha_2}}{\sqrt{1 - (\gamma\omega)^{\alpha_2+z}} \sqrt{1 - \omega^{2\alpha_2}}} - \frac{1}{\omega^{\alpha_2}} \right] + \frac{1}{\omega^{\alpha_2}} \right), \quad (2.8)$$

where the square bracket part is finite for $\alpha_2 > 0$ and

$$\omega = \frac{r}{r_t}, \quad \gamma = \frac{r_t}{r_H} < 1. \quad (2.9)$$

First, we compute the divergent part

$$\mathcal{A}_{div} = L^{d-1} r_t^{1-\alpha_2} \int_{\epsilon/r_t}^1 d\omega \frac{1}{\omega^{\alpha_2}} = L^{d-1} \frac{1}{\alpha_2 - 1} \frac{1}{\epsilon^{\alpha_2-1}}, \quad (2.10)$$

which is the same as the divergent contribution of the zero temperature background.

Now let us compute the finite part. At low temperature, we can evaluate the integral

$$l = r_t \int_0^1 d\omega \frac{\omega^{\alpha_2}}{\sqrt{1 - (\gamma\omega)^{\alpha_2+z}} \sqrt{1 - \omega^{2\alpha_2}}} \approx \sqrt{\pi} r_t \frac{\Gamma\left(\frac{1+\alpha_2}{2\alpha_2}\right)}{\Gamma\left(\frac{1}{2\alpha_2}\right)}, \quad (2.11)$$

and

$$\begin{aligned} \mathcal{A}_{fin} &\approx L^{d-1} r_t^{1-\alpha_2} \int_0^1 d\omega \frac{\omega^{-\alpha_2}}{\sqrt{1 - \omega^{2\alpha_2}}} \left(1 + \frac{1}{2} (\gamma\omega)^{\alpha_2+z} + \dots \right), \\ &= L^{d-1} l^{1-\alpha_2} c_\theta \left(-\frac{1}{\alpha_2 - 1} + \frac{\gamma^{\alpha_2+z}}{4\alpha_2} \frac{\Gamma\left(\frac{z+1}{2\alpha_2}\right)}{\Gamma\left(\frac{\alpha_2+z+1}{2\alpha_2}\right)} \frac{\Gamma\left(\frac{1}{2\alpha_2}\right)}{\Gamma\left(\frac{1+\alpha_2}{2\alpha_2}\right)} + \dots \right), \end{aligned} \quad (2.12)$$

which serves as an interpolating function from small temperature to high temperature. We evaluate it momentarily. At low temperature, the entanglement entropy for a strip in the general metric (2.1) is

$$\mathcal{S} = \frac{(RM_{Pl})^d}{4(\alpha_2 - 1)} \left(\left(\frac{\epsilon}{R_\theta} \right)^\theta \frac{L^{d-1}}{\epsilon^{d-1}} - c_\theta \left(\frac{l}{R_\theta} \right)^\theta \frac{L^{d-1}}{l^{d-1}} \left[1 - \tilde{c}_\theta (lT^{1/z})^{d+z-\theta} + \dots \right] \right), \quad (2.13)$$

where R_θ is a scale in which the hyperscaling violation becomes important and

$$c_\theta = \left(\frac{\sqrt{\pi} \Gamma\left(\frac{1+\alpha_2}{2\alpha_2}\right)}{\Gamma\left(\frac{1}{2\alpha_2}\right)} \right)^{\alpha_2}, \quad \tilde{c}_\theta = \frac{(\alpha_2 - 1)\sqrt{\pi}}{4\alpha_2 c_\theta} \frac{\Gamma\left(\frac{z+1}{2\alpha_2}\right)}{\Gamma\left(\frac{\alpha_2+z+1}{2\alpha_2}\right)} \left(\frac{4\pi}{|d+z-\theta|} \right)^{\frac{d+z-\theta}{z}}. \quad (2.14)$$

Thus we check that the entanglement entropy reduces to that of the zero temperature in the low temperature limit.

In the high temperature limit,

$$l = r_t \int^1 d\omega \frac{\omega^{\alpha_2}}{\sqrt{1 - (\gamma\omega)^{\alpha_2+z}} \sqrt{1 - \omega^{2\alpha_2}}} = r_t I_+(\gamma), \quad (2.15)$$

and

$$\mathcal{A} = L^{d-1} r_t^{1-\alpha_2} \int^1 d\omega \frac{\omega^{-\alpha_2}}{\sqrt{1 - (\gamma\omega)^{\alpha_2+z}} \sqrt{1 - \omega^{2\alpha_2}}} = L^{d-1} r_t^{1-\alpha_2} I_-(\gamma). \quad (2.16)$$

When $\gamma = \frac{r_t}{r_H} \rightarrow 1$, the integrals $I_+(\gamma)$ and $I_-(\gamma)$ are dominated by the contribution $\omega \approx 1$, and thus $I_+(\gamma) \approx I_-(\gamma) \approx l/r_H$ [8]. Thus

$$\mathcal{S}_{fin} \propto L^{d-1} l T^{(d-\theta)/z}, \quad (2.17)$$

which agrees with the thermal entropy, given in (2.4).

2.3 An explicit solution : EMD theories

In this section we would like to study an explicit solution with the properties described in the previous section. The explicit solution is given in [4] with two free parameters (γ, δ) in the context of EMD theories [63]-[74]. One of the main motivation of this section is to map the solution in terms of new parameters (z, θ) . We would like to examine the structures of the action and other fields associated with the metric with the hyperscaling violation with emphasis on 2 spatial dimensions in terms of those two parameters. In particular, we check whether the program to restrict the parameter space of the metric (2.1) using the null energy condition and positive specific heat constraint (allowed region (I)) is reasonable or not, by comparing to the previous efforts to do so using other means available in the literature [4], which include the information of the full solution, especially of the matter contents (allowed region (II)). We also generalize the solutions for the general dimensions in the following section §2.4.

The full set of near extremal solution for $d = 2$ is obtained with two parameters (γ, δ) [4]

$$\begin{aligned}
S &= \int d^{3+1}x \sqrt{-g} \left[R - \frac{e^{\gamma\phi}}{4} F_{\mu\nu} F^{\mu\nu} - \frac{1}{2} (\partial\phi)^2 - 2\Lambda e^{-\delta\phi} \right], \\
ds^2 &= -r(r-2m)r^{-4\frac{\gamma(\gamma-\delta)}{wu}} dt^2 + \frac{e^{\delta\phi} dr^2}{-w\Lambda r(r-2m)} + r^{2\frac{(\gamma-\delta)^2}{wu}} (dx^2 + dy^2), \\
e^\phi &= e^{\phi_0} r^{-4(\gamma-\delta)/(wu)}, \quad A_t = 2\sqrt{-v/(wu)} e^{-\frac{\gamma}{2}\phi_0} (r-2m), \\
wu &= 3\gamma^2 - \delta^2 - 2\gamma\delta + 4, \quad u = \gamma^2 - \gamma\delta + 2, \quad v = \delta^2 - \gamma\delta - 2.
\end{aligned} \tag{2.18}$$

This metric was constructed to get a general scaling solution in IR, and physical properties such as energy, entropy and conductivities show power law behaviors, characteristic features of scaling invariant theories. An important difference is that the hyperscaling property is violated. Lifshitz solutions are special cases for $\gamma = -\sqrt{4/(z-1)}$ and $\delta = 0$. This solution provides the most general IR asymptotics at finite density with a single gauge field A and a Dilaton field ϕ , and is embedded in higher dimensional AdS or Lifshitz spacetimes [5].

Using the coordinate transform

$$r \rightarrow \tilde{b} r^{\tilde{a}}, \quad 2m = \tilde{b} r_H^{\tilde{a}}, \quad \tilde{a} = -\frac{wu}{\gamma^2 - \delta^2}, \quad \tilde{b} = \left(\frac{-w\Lambda}{\tilde{a}^2 e^{\delta\phi_0}} \right)^{\tilde{a}/2}, \tag{2.19}$$

the metric can be recast into

$$ds^2 = r^{-2+2\theta/d} \left(-r^{-2(z-1)} f(r) dt^2 + \sum_{i=1}^d dx_i^2 + \frac{dr^2}{f(r)} \right), \tag{2.20}$$

$$f = 1 - \frac{2m/\tilde{b}}{r^{\tilde{a}}} = 1 - \left(\frac{r}{r_H} \right)^{\frac{wu}{\gamma^2 - \delta^2}} = 1 - \left(\frac{r}{r_H} \right)^{d+z-\theta}, \tag{2.21}$$

where we are able to put $\tilde{b} = 1$ with a suitable choice of Λ or ϕ_0 as $e^{\delta\phi_0} = \frac{-w\Lambda}{\tilde{a}^2}$, and the coefficient of dt^2 term becomes unity. The parameters z and θ are the dynamical and hyperscaling violation exponents, respectively. Explicitly, they are identified as follows in terms of γ, δ for $d = 2$

$$\theta = \frac{4\delta}{\gamma + \delta}, \quad z = 1 + \frac{2\delta}{\gamma + \delta} + \frac{4}{\gamma^2 - \delta^2}. \tag{2.22}$$

From these we check the relation $d + z - \theta = -\tilde{a} = \frac{wu}{\gamma^2 - \delta^2}$. Thus we can translate all the results of [4] in terms of z and θ . Again, we check that $\delta = 0$ is a Lifshitz solution. In turn, we have the relations

$$\gamma = \pm \frac{4 - \theta}{\sqrt{-4 + 4z - 2z\theta + \theta^2}}, \quad \delta = \pm \frac{\theta}{\sqrt{-4 + 4z - 2z\theta + \theta^2}}, \quad \frac{\gamma}{\delta} = \frac{4 - \theta}{\theta}. \tag{2.23}$$

It is desirable to examine the metric and other fields more closely. For this purpose, we completely rewrite this solution in terms of the parameter z and θ .

$$S = \int d^4x \sqrt{-g} \left[R - \frac{Z}{4} F_{\mu\nu} F^{\mu\nu} - \frac{1}{2} (\partial\phi)^2 + V \right], \quad (2.24)$$

$$ds^2 = r^{-2+\theta} \left(-r^{-2(z-1)} f(r) dt^2 + \sum_{i=1}^2 dx_i^2 + \frac{dr^2}{f(r)} \right), \quad (2.25)$$

$$e^\phi = r^s, \quad s = \pm \sqrt{-4 + 4z - 2z\theta + \theta^2}, \quad (2.26)$$

$$V = V_0 e^{-\frac{\theta}{s}\phi}, \quad V_0 = (2 + z - \theta)(1 + z - \theta), \quad (2.27)$$

$$Z = \frac{1}{q^2} e^{\frac{4-\theta}{s}\phi}, \quad A_t = q \sqrt{\frac{2z-2}{z+2-\theta}} r^{-2-z+\theta} f(r), \quad (2.28)$$

$$f(r) = 1 - \left(\frac{r}{r_H} \right)^{2+z-\theta}. \quad (2.29)$$

Note that we set $\tilde{b} = 1$ using Λ .⁷ The remaining constant ϕ_0 serves as an integration constant. The two solutions are corresponding to the sign of the relation (2.23). From the Maxwell equation $\partial_\mu (\sqrt{-g} Z F^{\mu\nu}) = 0$, we introduce an integration constant $Q = \sqrt{-g} Z F^{\mu\nu}$, which is identified as a charge density. In terms of q , it is expressed as $Q = -\sqrt{2(z-1)(2+z-\theta)}/q$. We check explicitly that this satisfy the Einstein equation, and the scalar equation is automatically satisfied. Under the scaling transformation

$$t \rightarrow \lambda^z t, \quad x_i \rightarrow \lambda x_i, \quad r \rightarrow \lambda r, \quad (2.30)$$

the dilaton, the vector potential and metric transform as

$$\phi \rightarrow \pm \sqrt{4(z-1) + \theta(\theta - 2z)} \log(\lambda) + \phi, \quad (2.31)$$

$$A \rightarrow \lambda^{\theta-2} A, \quad (2.32)$$

$$ds \rightarrow \lambda^{\theta/d} ds, \quad (2.33)$$

while the action remains invariant under the scaling transformation. These properties for the dilaton and vector potential were noticed in [13].

It is interesting to consider various special cases. For $\theta = 4$, the gauge field and the dilaton become decoupled. If we put $\theta = 0$, the potential V becomes a constant. The

⁷We are grateful to Sang-Jin Sin and Yunseok Seo for the fruitful discussions and comments on the metric, gauge field and the associated charge in terms of (θ, z) .

solution becomes nothing but the Lifshitz type supported by a gauge field and a scalar.

$$S = \int d^4x \sqrt{-g} \left[R - \frac{Z}{4} F_{\mu\nu} F^{\mu\nu} - \frac{1}{2} (\partial\phi)^2 + V_0 \right], \quad (2.34)$$

$$ds^2 = r^{-2} \left(-r^{-2(z-1)} f(r) dt^2 + \sum_{i=1}^2 dx_i^2 + \frac{dr^2}{f(r)} \right), \quad (2.35)$$

$$V_0 = (2+z)(1+z), \quad e^\phi = r^s, \quad s = \pm\sqrt{4z-4}, \quad (2.36)$$

$$Z = \frac{1}{q^2} e^{4\phi/s}, \quad A_t = q \sqrt{\frac{2z-2}{z+2}} r^{-2-z} f(r), \quad (2.37)$$

$$f(r) = 1 - \left(\frac{r}{r_H} \right)^{2+z}. \quad (2.38)$$

In this form, the scalar potential becomes a constant, which can be identified as a cosmological constant term for 3 + 1 dimensional gravity system. If we further restrict to $z = 1$, the metric becomes

$$S = \int d^4x \sqrt{-g} [R + 6], \quad (2.39)$$

$$ds^2 = r^{-2} \left(-f(r) dt^2 + \sum_{i=1}^2 dx_i^2 + \frac{dr^2}{f(r)} \right), \quad (2.40)$$

which is the usual AdS solution. A particular case $z = 1, \theta \neq 0$ is supported by the dilaton only because the gauge field vanishes.

Alternative

Using the coordinate transform

$$r \rightarrow \tilde{b} u^{\tilde{a}}, \quad \tilde{a} = \frac{wu}{\gamma^2 - \delta^2}, \quad \tilde{b} = \left(\frac{-w\Lambda}{\tilde{a}^2 e^{\delta\phi_0}} \right)^{-\tilde{a}/2} = 1, \quad (2.41)$$

the metric can be recast into

$$ds^2 = u^{2-2\theta/d} \left(-u^{2(z-1)} f(u) dt^2 + \sum_{i=1}^d dx_i^2 + \frac{du^2}{u^4 f(u)} \right), \quad (2.42)$$

$$f = 1 - \frac{2m/\tilde{b}}{u^{\tilde{a}}} = 1 - \left(\frac{u_H}{u} \right)^{\frac{wu}{\gamma^2 - \delta^2}} = 1 - \left(\frac{u_H}{u} \right)^{d+z-\theta}, \quad (2.43)$$

where z and θ are the dynamical and hyperscaling violation exponents, respectively. Explicitly, they are identified as follows in terms of γ, δ for $d = 2$

$$\theta = \frac{4\delta}{\gamma + \delta}, \quad z = 1 + \frac{2\delta}{\gamma + \delta} + \frac{4}{\gamma^2 - \delta^2}. \quad (2.44)$$

Thus we explicitly check the alternative coordinate system does not change the dynamical z and hyperscaling violation exponent θ .

2.3.1 Thermodynamics

As a complete solution is given in (2.24), we would like to also list thermodynamic quantities. These are computed in [4] using the Euclidean action with appropriate boundary terms. We can view this section as a two parameter generalization in terms of (z, θ) of the AdS₄ black hole for $(z = 1, \theta = 0)$.

The temperature and entropy are given by

$$T = \frac{1}{4\pi} \sqrt{-w\Lambda} e^{-\frac{\delta}{2}\phi_0} (2m)^{1-2\frac{(\gamma-\delta)^2}{wu}} = \frac{(2+z-\theta)}{4\pi} r_H^{-z}, \quad (2.45)$$

$$S = \frac{\Omega_2}{4} (2m)^{2\frac{(\gamma-\delta)^2}{wu}} = \frac{\Omega_2}{4} r_H^{-2+\theta}, \quad \sim T^{\frac{2-\theta}{z}}. \quad (2.46)$$

Note the temperature vanishes in the $r_H \rightarrow \infty$ limit if and only if the dynamical exponent z is positive, and the entropy vanishes as $r_H \rightarrow \infty$ for $\theta < 2$. These two observations support further restriction of the allowed regions (I) to the bottom right one in the figure 1, together with the result of the entanglement entropy analysis. We observe that $\theta = 2$, for $d = 2$, is special. The entropy stays finite for this case, which corresponds to the case $\gamma = \delta$. And the geometry turns out to be a direct product AdS₂ \times S^2 in the extremal limit $m = 0$. This is clear from the geometry given in (2.18).

The energy is

$$E = \frac{\Omega_2}{4\pi} \sqrt{\frac{-\Lambda}{wu^2}} (\gamma - \delta)^2 m = \frac{\Omega_2}{4\pi} \frac{2-\theta}{4} r_H^{-2-z+\theta}. \quad (2.47)$$

Notice that the mass is identically zero for $\theta = 2$, which is again the case with the geometry AdS₂ \times S^2 .

For the canonical ensemble, where the temperature is allowed to vary and the charge density is fixed, the Helmholtz potential is given by

$$W = -\frac{\Omega_2}{8\pi} \sqrt{-w\Lambda} e^{-\frac{\delta}{2}\phi_0} \left[1 - 2\frac{(\gamma-\delta)^2}{wu} \right] m = -\frac{\Omega_2}{16\pi} z r_H^{-2-z+\theta}. \quad (2.48)$$

Finally the heat capacity is found to be

$$C_Q = \frac{\Omega_2}{4} \frac{2(\gamma-\delta)^2}{wu} \left[1 - 2\frac{(\gamma-\delta)^2}{wu} \right]^{-1} \left(e^{\frac{\delta}{2}\phi_0} \frac{4\pi T}{\sqrt{-w\Lambda}} \right)^{\frac{2(\gamma-\delta)^2}{wu-2(\gamma-\delta)^2}}, \quad (2.49)$$

$$= \frac{\Omega_2}{4} \frac{2-\theta}{z} \left(\frac{4\pi T}{2+z-\theta} \right)^{\frac{2-\theta}{z}}. \quad (2.50)$$

Thus the positive heat capacity gives a condition $\frac{2-\theta}{z} > 0$, which is consistent with (2.3) for $d = 2$.

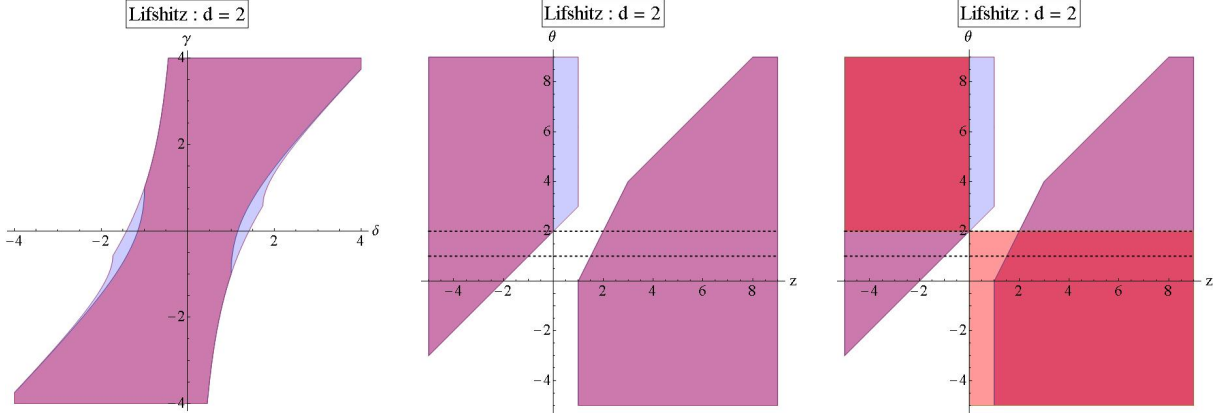


Figure 2: The left plot shows the allowed regions for the Lifshitz geometry in terms of the parameters γ and δ . The outer blue regions are allowed by the Gubser’s criteria, while the inner purple region is allowed after taking into account of the other constraints including the well defined spectrum [4][51][52][71]. The middle plot is the same as the left plot in terms of the parameters z and θ , where the middle blue region is allowed by Gubser’s criteria, for example. The right plot shows the allowed regions after taking into account of the specific heat condition (2.3), where the two red regions, top-left and bottom-right regions are allowed (allowed region (II)). It is very interesting to confirm that these allowed regions (II) are the same as those of the middle plot, allowed region (I), in Fig. (1).

2.3.2 Constraints on the parameter space

Using the low energy effective holographic approach, consistent regions in the parameter spaces (γ, δ) of the solution (2.18) are analyzed in [4][51][52][71]. Major constraints are the Gubser’s bound, excluding naked singularities if the scalar potential is not bound below upon evaluating in the solution [75][78][79], as well as well defined spin 1 and spin 2 fluctuations around the singularity [80]. These constraints on the (γ, δ) parameter spaces are depicted in the left plot of figure 2. Using the relation (2.22) or (2.23), we can re-express this constraints in terms of (z, θ) , which is depicted in the middle plot. Finally the allowed regions are severely constrained by the positive specific heat constraint, which is the purple regions in the figure 2. This can be compared to that of the middle plot in figure 1. Interestingly, these two results show the same allowed regions.⁸

This demonstrate the success of the program, which classify the low energy and lower dimensional holographic theories in terms of the metrics with the parameters (z, θ) and constrain the allowed parameter spaces using the null energy conditions as well as some thermodynamic stability constraints. Allowed region (I) is restricted, mainly, from the metric, while allowed region (II) is constrained also from matter contents of the full solution.

⁸We are grateful to Elias Kiritsis for discussions and comments on the related subjects.

2.4 $d + 2$ dimensional EMD solutions

In this section, we consider the explicit EMD solution for arbitrary number of spatial dimensions constructed in [4] and rewrite the solution in terms of the parameters (z, θ) . By doing so, we confirm that the emblackening factor has the same form at finite temperature.

The full set of near extremal solution for general d spatial dimensions is obtained in [4]

$$\begin{aligned}
S &= \int d^{d+2}x \sqrt{-g} \left[R - \frac{e^{\gamma\phi}}{4} F_{\mu\nu} F^{\mu\nu} - \frac{1}{2} (\partial\phi)^2 - 2\Lambda e^{-\delta\phi} \right], \\
ds^2 &= \left(\frac{\tilde{r}}{\ell} \right)^{\frac{(\gamma-\delta)^2}{d}} \left[-\tilde{f}(\tilde{r}) dt^2 + \sum_{i=1}^d dx_i dx^i \right] + \frac{d\tilde{r}^2}{\tilde{f}(\tilde{r})}, \\
\tilde{f}(\tilde{r}) &= \frac{8d\ell^2 (-\Lambda) e^{-\delta\phi_0}}{u^2 w} \left(\frac{\tilde{r}}{\ell} \right)^{1 - \frac{(d+1)(\gamma-\delta)^2}{2d}} \left[\left(\frac{\tilde{r}}{\ell} \right)^{\frac{wu}{2d}} - 2m \right], \\
e^\phi &= e^{\phi_0} \left(\frac{\tilde{r}}{\ell} \right)^{(\delta-\gamma)}, \quad A_t = \frac{4d}{wu} \sqrt{\frac{\ell^2 \Lambda v}{u}} e^{-\frac{(\gamma+\delta)}{2}\phi_0} \left[\left(\frac{\tilde{r}}{\ell} \right)^{\frac{wu}{2d}} - 2m \right], \\
wu &= 2d + (d+1)\gamma^2 - 2\gamma\delta - (d-1)\delta^2, \quad u = \gamma^2 - \gamma\delta + 2, \quad v = \delta^2 - \gamma\delta - 2.
\end{aligned} \tag{2.51}$$

One can readily check that this general metric reduces to the $d = 2$ solution (2.18), and similar properties listed there also apply to this metric.

Using the coordinate transform

$$\tilde{r} \rightarrow br^a, \quad a = -\frac{2d}{(\gamma + (d-1)\delta)(\gamma - \delta)}, \tag{2.52}$$

$$b = \left(\frac{\tilde{f}_0}{a^2} \right)^{\frac{a}{2}} \ell^{1-a}, \quad \tilde{f}_0 = \frac{8d\ell^2 (-\Lambda) e^{-\delta\phi_0}}{u^2 w}, \tag{2.53}$$

the metric can be recast into

$$ds^2 = r^{-2+2\theta/d} \left(-a^2 \ell^2 r^{-2(z-1)} f(r) dt^2 + \sum_{i=1}^d dx_i^2 + \frac{dr^2}{f(r)} \right), \tag{2.54}$$

$$f = 1 - 2m \left(\frac{br^a}{\ell} \right)^{-\frac{wu}{2d}} = 1 - \left(\frac{r}{r_H} \right)^{\frac{wu}{(\gamma+(d-1)\delta)(\gamma-\delta)}} = 1 - \left(\frac{r}{r_H} \right)^{d+z-\theta}, \tag{2.55}$$

where we use Λ or ϕ_0 to set $b/\ell = 1$ as

$$2(-\Lambda) e^{-\delta\phi_0} = \frac{u^2 w a^2}{4d}, \tag{2.56}$$

Explicitly, the exponents are identified as follows in terms of γ, δ for $d + 2$ dimensional solution

$$\theta = \frac{d^2 \delta}{\gamma + (d-1)\delta}, \quad z = 1 + \frac{d\delta}{\gamma + (d-1)\delta} + \frac{2d}{(\gamma - \delta)(\gamma + (d-1)\delta)}. \tag{2.57}$$

In turn we have

$$\gamma = \frac{\pm\sqrt{2}(d^2 - d\theta + \theta)}{\sqrt{-d^3 + d^3z - d^2z\theta + d\theta^2}}, \quad \delta = \frac{\pm\sqrt{2}\theta}{\sqrt{-d^3 + d^3z - d^2z\theta + d\theta^2}}. \quad (2.58)$$

Thus we can translate all the parameters in terms of z and θ . For example, we get

$$2(-\Lambda)e^{-\delta\phi_0} = \frac{u^2wa^2}{4d} = (d + z - \theta - 1)(d + z - \theta). \quad (2.59)$$

The resulting solutions has the following form

$$S = \int d^{d+2}x \sqrt{-g} \left[R - \frac{Z}{4} F_{\mu\nu} F^{\mu\nu} - \frac{1}{2} (\partial\phi)^2 + V \right], \quad (2.60)$$

$$ds^2 = r^{-2+2\theta/d} \left(-r^{-2(z-1)} f(r) dt^2 + \sum_{i=1}^d dx_i^2 + \frac{dr^2}{f(r)} \right), \quad (2.61)$$

$$e^\phi = r^s, \quad s = \pm\sqrt{2(1-\theta/d)(d(z-1)-\theta)}, \quad (2.62)$$

$$V = V_0 e^{-\frac{2\theta}{sd}\phi}, \quad V_0 = (d + z - \theta - 1)(d + z - \theta), \quad (2.63)$$

$$Z = \frac{1}{q^2} e^{\frac{2(d^2-(d-1)\theta)}{sd}\phi}, \quad (2.64)$$

$$A_t = q \sqrt{\frac{2(z-1)}{d+z-\theta}} r^{-d-z+\theta} f, \quad (2.65)$$

$$f = 1 - \left(\frac{r}{r_H} \right)^{d+z-\theta}, \quad (2.66)$$

where we absorb the dimensionful factor by changing coordinate $aldt \rightarrow dt$ and identify $q = e^{-\frac{\gamma}{2}\phi_0}$. For other useful information, especially for $d = 2$, can be found in the previous section, near the equation (2.24).

3 Theories with Schrödinger scaling I

Let us consider first the Schrödinger backgrounds, whose field theory duals have Schrödinger symmetry, initiated in [81][82] for the case $\theta = 0$. The holographic dictionary turns out to be drastically different from that of the Lifshitz case. There are more than one holographic direction, and $d+3$ dimensional gravity backgrounds with Schrödinger isometry corresponds to $d+1$ dimensional field theories. There are two light-cone coordinates: one has the role of time, while the other supply the dual particle number \mathcal{M} .⁹ Their finite temperature generalizations are considered in [83]-[87] using the null Melvin twist [88][89]. See also further string theory related solutions in [90]-[105]. In this section, we concentrate on a very

⁹ The role of the light-cone coordinate ξ has not been fully appreciated in the context of holography. See some developments along this line in [106][107], where \mathcal{M} is generalized to be complex in the context of time

nice paper [90], which worked out many different non-relativistic backgrounds using the null Melvin twist.

At zero temperature, the theories with Schrödinger scaling symmetry are described by the metric (1.1) with $b = 1$, $a = 1$ and $D = d + 1$

$$ds^2 = r^{-2+\frac{2\theta}{d+1}} \left(-r^{-2(z-1)} dt^2 - 2 dt d\xi + dr^2 + \sum_{i=1}^c dx_i^2 + \sum_{j=c+1}^d \eta_j(r, t, \vec{x}) dx_j^2 \right). \quad (3.2)$$

This metric is extensively analyzed in [11] for both cases with and without hyperscaling violation exponent. In particular, a prescription for minimal surfaces of this “codimension 2 holography,” is proposed to demonstrate the $(d-1)$ dimensional area law for the entanglement entropy starting from $(d+3)$ dimensional Schrödinger backgrounds. Surprisingly, the area law is violated for $d+1 < z < d+2$ due to the contribution of the spectator coordinate ξ , even without hyperscaling violation. See [17] for the top-down approach for the hyperscaling violation theories with Schrödinger backgrounds.

The program to restrict the parameter space of (z, θ) of the metric (3.2) for given spatial dimensions d is carried out with the null energy condition. These are depicted in figure 1 and 2 of [11]. We observe a clear distinction, compared to the theories with Lifshitz scaling, that the entanglement entropy condition as well as null energy condition have non-trivial dependence on z . For example, the entanglement entropy shows an extensive violation of the area law, being proportional to volume, for $\theta = d + 2 - z$. Thus we expect to exclude the parameter spaces for $\theta > d + 2 - z$ from the analysis of entanglement entropy. We further investigate several different string theory solutions in Appendix §B. Thus, the program equally works for the theories with Schrödinger scaling at zero temperature.

Naively, we desire to find the most general metrics with Schrödinger scaling at finite temperature with the hyperscaling violation exponent θ only using the radial coordinates similar to the Lifshitz case discussed in §2. We quickly realize that this attempt is bound to fail due to the dimensionful parameter, b , which is present in the known Schrödinger black hole solutions [83]-[87]. This parameter is intrinsically different from other dimensionful parameters because it actually serves as a thermodynamic variable in the black hole thermodynamics. Thus b can not be absorbed in the overall dependence associated with θ or in other coordinates without altering the physical properties of the original solutions. It is difficult to

dependent setup. There one considers a slightly more general metric for $\theta = 0$ and $\sharp = 1$ as

$$ds^2 = r^{-2} \left(-g(r, t) dt^2 - 2 dt d\xi + dr^2 + \sum_{i=1}^d dx_i^2 + h(r, t) dr dt \right). \quad (3.1)$$

Two time correlation functions have been constructed to show slow dynamics, power law decaying behavior in [106] for the pure imaginary \mathcal{M} . Their logarithmic extension is investigated in [107] to seek connections to the Kardar-Parisi-Zhang universality class. See also [108][109] for different considerations.

constrain the most general Schrödinger invariant metric, because there are many different scaling invariant combinations one can construct using r and b . Because of this, we change our strategy to investigate the theories with a Schrödinger isometry at finite temperature.

We concentrate on the non-relativistic Dp branes solutions [90] at finite temperature as our prime examples and dimensionally reduce them to understand their physical properties in §3.1. By doing so, we explicitly check whether we can trust the naively constructed effective holographic theories with Schrödinger isometry. In particular, we determine the dynamical exponent of the non-relativistic Dp branes solutions in §3.1.1, which turns out to be a non-trivial task. We investigate other physical properties including thermodynamics in the rest of the section §3.1. While doing this investigation, we find an important technical reason for the earlier observation that the thermodynamic properties of the Schrödinger backgrounds are identical to those of the ALCF. We study the finite temperature entanglement entropy in §3.2. There we explicitly check that the entanglement entropy cross over to the thermal entropy in the high temperature limit, while it reproduces the zero temperature entanglement entropy in the small temperature limit. Then we consider the effective approach based on the results of the dimensional reduction in §3.3.

We separately consider the other geometries with Schrödinger scaling, ALCF, in the following section §4 because they give fairly different looking physical properties at finite temperature.

3.1 String theory realizations of Schrödinger backgrounds

Let us consider the following non-relativistic Dp branes solutions [90], constructed from the black Dp brane solutions [110][111] using the null Melvin twist [88][89]. The metric can be written in a slightly more organized form as

$$ds_{Dp}^2 = \frac{1}{h} \left[-\frac{f}{b^2(1-f)} dt^2 + \frac{b^2(1-f)}{K} \left(d\xi - \frac{1+f}{(1-f)2b^2} dt \right)^2 + \sum_{i=1}^{p-1} dx_i^2 \right] + h \left[\frac{1}{f} d\rho^2 + \rho^2 \left(\frac{1}{K} (d\chi + \mathcal{A})^2 + ds_{\mathbb{P}^2}^2 \right) \right], \quad (3.3)$$

$$e^\Phi = \left(\frac{h^{3-p}}{K} \right)^{1/2}, \quad K = 1 + b^2 \rho^2 \left(\frac{\rho_H}{\rho} \right)^{7-p}, \quad (3.4)$$

$$B = \frac{\rho^2}{K} (d\chi + \mathcal{A}) \wedge \left(\frac{1+f}{2} dt - b^2(1-f) d\xi \right), \quad (3.5)$$

$$h^2 = 1 + \left(\frac{\rho_p}{\rho} \right)^{7-p}, \quad f(\rho) = 1 - \left(\frac{\rho_H}{\rho} \right)^{7-p}. \quad (3.6)$$

We consider the near horizon geometry with $h \rightarrow \left(\frac{\rho_p}{\rho} \right)^{(7-p)/2}$, followed by the change

of coordinate $\rho = 1/u$, followed by the compactification of the solution down to $(p + 2)$ dimensions. Dimensional reduction to $p + 2$ dimensions and going to Einstein frame give

$$ds^2 = r^{-\frac{2(9-p)}{p(5-p)}} K^{\frac{1}{p}} \left[\frac{-f}{b^2(1-f)} dt^2 + \frac{b^2(1-f)}{K} \left(d\xi - \frac{1+f}{2b^2(1-f)} dt \right)^2 + \sum_{i=1}^{p-1} dx_i^2 + \frac{dr^2}{f} \right], \quad (3.7)$$

$$K = 1 + c b^2 r_H^{-2\frac{7-p}{5-p}} r^2, \quad f = 1 - \left(\frac{r}{r_H} \right)^{\frac{2(7-p)}{5-p}}, \quad (3.8)$$

where we use $u = \left(\frac{2}{5-p} \right)^{-\frac{2}{5-p}} u_p^{\frac{7-p}{5-p}} r^{\frac{2}{5-p}}$ and $c = \left(\frac{2}{5-p} \right)^{\frac{4}{5-p}} u_p^{-2\frac{7-p}{5-p}}$. With this form at hand, we realize that the thermodynamic properties, related to the horizon such as temperature and entropy, of the Schrödinger type solutions are independent of K . This is an important technical detail that verify the earlier claims that the thermodynamics of the Schrödinger type theories are identical to those of the ALCF [83][84][112]. This is checked explicitly in §3.1.2 below.

Thus the non-relativistic Dp brane solutions (3.3) gives the Schrödinger type theories with hyperscaling violation with the identifications

$$\theta = p - \frac{9-p}{5-p} = -\frac{(p-3)^2}{5-p}, \quad (3.9)$$

where we use $D = p = d + 1$. Note that the overall dimensionful parameter only contains u_p , which is important to provide a unique physical meaning to the hyperscaling violation exponent, without being mixed with the other thermodynamic parameters, b and r_H .

3.1.1 Determination of the dynamical exponent

Here we would like to identify the dynamical exponent in terms of the parameter p by taking the zero temperature limit carefully. There is actually a subtle point.

At first glance, it is tempting to use the ADM form of the metric (3.7) to identify the dynamical exponent from the first term with dt^2 .

$$\frac{-f}{b^2(1-f)} dt^2 = \left[b^{-2} r_H^{\frac{2(7-p)}{5-p}} \right] r^{-\frac{2(7-p)}{5-p}} (-f dt^2). \quad (3.10)$$

Naively, we can identify the dynamical exponent in terms of the radial dependence by absorbing all the dimensionful parameters into t by redefining $t \rightarrow br_H^{-\frac{(7-p)}{5-p}} t$. Then we get

$$z' = \frac{12-2p}{5-p}, \quad (3.11)$$

Seemingly, it is consistent with the fact that $K \approx 1$ is not important because of the physically relevant range $0 \leq r \leq r_H$. But this identification is not consistent with that of the zero temperature Schrödinger background due to a subtle cancellation involved with a subleading term in K .¹⁰

Let us identify the dynamical exponent using a slightly different form of the metric (3.7)

$$ds^2 = r^{-2+\frac{2\theta}{p}} \left(\frac{(1+f)^2 - 4fK}{4b^2(1-f)K} dt^2 + \frac{b^2(1-f)}{K} d\xi^2 - \frac{1+f}{K} dt d\xi + \sum_{i=1}^{p-1} dx_i^2 + \frac{dr^2}{f} \right). \quad (3.12)$$

Let us take a zero temperature limit, $r_H \rightarrow \infty$, or asymptotic form at the boundary, $r \rightarrow 0$.

$$ds^2 = r^{-2+2\theta/p} \left(-cr^{\frac{-4}{5-p}} dt^2 - 2dt d\xi + \sum_{i=1}^{p-1} dx_i^2 + \frac{dr^2}{f} \right). \quad (3.13)$$

The constant c in front of the term dt^2 can be absorbed by redefining t and ξ . Thus we should identify the dynamical exponent

$$2 - 2z = \frac{-4}{5-p} \quad \longrightarrow \quad z = \frac{7-p}{5-p}, \quad (3.14)$$

to be in consistent with the zero temperature background. In turn, we can identify z' in terms of z as

$$z' = \frac{12-2p}{5-p} = z + 1. \quad (3.15)$$

Thus z is the correct dynamical exponent we are going to use in this section because it is consistent with the zero temperature limit. As a byproduct, we identify the parameter β in terms of c as

$$c = \left(\frac{2}{5-p} \right)^{\frac{4}{5-p}} u_p^{-2\frac{7-p}{5-p}}, \quad (3.16)$$

which is independent of the parameters b and the horizon radius related to the temperature.

Note there are three different dimensionful parameters, u_p , b and u_H , in the Schrödinger metric at finite temperature. We can pull out u_p to be an overall factor by redefining coordinates, and it contributes to the part related to the hyperscaling violation. The other two are physical parameters, being two independent thermodynamic variables, which are

¹⁰If one include the scaling dimension of b for the identification of z from (3.10), he or she would get the correct value. Our motivation starts from the low energy effective description without knowing precise information on b and thus handling the parameter would be an important task.

important to keep track. In this sense, z in equation (3.14) is well established because the physical parameters b and u_H are not involved in the identification process. On the other hand, we need to be careful for the identification of (3.11) because it requires to redefine $t \rightarrow br_H^{-\frac{(7-p)}{5-p}} t$. The latter case would change or lose some physical information because the coordinate redefinition is temperature dependent. (see related motivation in footnote 10.)

3.1.2 Thermodynamic Properties

Thermodynamic properties of the metric (3.12) are more transparent in the ADM form (3.7). We can read off the lapse function N , the shift function V^i and the horizon coordinate velocity in the x^- direction Ω_H , which can be interpreted as chemical potential associated with a conserved quantity along the x^- direction.

$$N = r^{-\frac{9-p}{p(5-p)}} \sqrt{\frac{f}{(1-f)b^2}}, \quad V^- = -\frac{1}{2b^2} \frac{1+f}{1-f}, \quad \Omega_H = \frac{1}{2b^2}. \quad (3.17)$$

Some of the thermodynamic properties can be directly analyzed using the horizon properties. Temperature, entropy and chemical potential along the ξ direction are given by

$$T = \frac{1}{2\pi br_H} \left| \frac{7-p}{5-p} \right|, \quad S_T \approx br_H^{-\frac{9-p}{5-p}} V_{p-1} V_\xi, \quad \Omega = \frac{1}{2b^2}. \quad (3.18)$$

Note that the entropy is independent of K , as explained above. There is a hidden dimensional parameters R_θ in the entropy expression. Assuming the front factor in metric (3.7) being $\left(\frac{r}{R}\right)^{-2} \left(\frac{r}{R_\theta}\right)^{2\theta/p}$, the entropy becomes $S_T = \frac{(M_{pl}R)^p}{4} R_\theta^{-\theta} V_{p-1} V_\xi br_H^{-\frac{9-p}{5-p}}$.

3.1.3 Reduction to Lifshitz type theories

It is interesting to connect to the Schrödinger type theories to Lifshitz type theories in one way or another because the properties of the latter might shed some light to the former. Here we just formally identify the exponents of the Schrödinger theories to that of the Lifshitz theories by dimensionally reducing (3.7) along ξ coordinate.

The resulting $p+1$ dimensional Lifshitz type solution has the following metric in Einstein frame

$$ds^2 = r^{-\frac{4}{(p-1)(5-p)}} \left(br_H^{-\frac{7-p}{5-p}} \right)^{\frac{2}{p-1}} \left[\frac{-f}{b^2 r_H^{-\frac{2(7-p)}{5-p}}} r^{-\frac{2(7-p)}{5-p}} dt^2 + \sum_{i=1}^{p-1} dx_i^2 + \frac{dr^2}{f} \right], \quad (3.19)$$

where the metric has the same emblackening factor $f = 1 - \left(\frac{r}{r_H}\right)^{\frac{2(7-p)}{5-p}}$, which still has the pivotal role for the identification of the dynamical exponent as in the Schrödinger case.

Note that the front factor $K^{\frac{1}{p}}$ cancels out the contribution from reduced ξ coordinate. The dimensionful parameters in the term dt^2 can be absorbed by the coordinate redefinition.¹¹ Thus we identify

$$\theta_{LF} = -\frac{p^2 - 6p + 7}{5 - p}, \quad z_{LF} = \frac{12 - 2p}{5 - p}. \quad (3.20)$$

We would like to point out that the emblackening factor becomes

$$d + z - \theta = \frac{2(7 - p)}{5 - p}, \quad f = 1 - \left(\frac{r}{r_H}\right)^{d+z-\theta}, \quad (3.21)$$

which shares the same property of the general theories with Lifshitz isometry advertised in §2.1.

3.2 Entanglement entropy

We would like to evaluate the entanglement entropy for the Schrödinger backgrounds at finite temperature described by the metric (3.7)

$$ds^2 = r^{\frac{2\theta}{p}-2} K^{\frac{1}{p}} \left[\frac{-f dt^2}{(1-f)b^2} + \frac{(1-f)b^2}{K} \left(d\xi - \frac{1+f}{1-f} \frac{dt}{2b^2} \right)^2 + \sum_{i=1}^{p-1} dx_i^2 + \frac{dr^2}{f} \right],$$

$$f = 1 - \left(\frac{r}{r_H}\right)^{2z}, \quad K = 1 + \beta b^2 r_H^{-2z} r^2, \quad (3.22)$$

where $D = p = d + 1$ and $\beta = \left(\frac{2}{5-p}\right)^{\frac{4}{5-p}} u_p^{-2z} = (z-1)^{2(z-1)} u_p^{-2z}$. Note that we use θ, z just for the notational simplicity in this section. They are given by

$$\theta = -\frac{(p-3)^2}{5-p}, \quad z = \frac{7-p}{5-p}. \quad (3.23)$$

The entanglement entropy of the metric (4.18) with finite temperature can be computed for a strip with ξ direction

$$0 \leq \xi \leq L_\xi, \quad -l \leq x_1 \leq l, \quad 0 \leq x_i \leq L, \quad i = 2, \dots, p-1 \quad (3.24)$$

in the limit $l \ll L, L_\xi$. The strip is located at $r = \epsilon$, and the profile of the surface in the bulk is given by $r = r(x_1)$. The minimal surface has turning point at $r = r_t$. Thus, to get the entanglement entropy, we evaluate the following expression

$$l = \int_0^{r_t} dr \frac{1}{\sqrt{f}} \frac{(r/r_t)^{\alpha_2} (K(r)/K(r_t))^{p/2p-1/2}}{\sqrt{1 - (r/r_t)^{2\alpha_2} (K(r)/K(r_t))^{p/p-1}}}, \quad (3.25)$$

¹¹We further assume that $br_H^{-\frac{7-p}{5-p}} = 1$ upon taking the dimensional reduction along the coordinate ξ . The thermodynamic properties of the Lifshitz space are expected to be independent of the parameter b , and the resulting Lifshitz metric is also expected to be independent of r_H .

and

$$\mathcal{A} = L^{p-2} L_\xi \int_\epsilon^{r_t} dr \frac{1}{\sqrt{f}} \frac{(br_H^{-z}) r^{-\alpha_2} K(r)^{-p/2p+1/2}}{\sqrt{1 - (r/r_t)^{2\alpha_2} (K(r)/K(r_t))^{p/p-1}}}, \quad (3.26)$$

where $\alpha_2 = p - z - \theta$. Note that the expression is independent of K because the front factor $K^{1/p}$ multiplied by p times cancel $1/K$ in front of $d\xi^2$. Thus the entanglement entropy of the Schrödinger black hole is identical to that of the ALCF, which is discussed in the following section. Thus we get

$$l = \int_0^{r_t} dr \frac{1}{\sqrt{f}} \frac{(r/r_t)^{\alpha_2}}{\sqrt{1 - (r/r_t)^{2\alpha_2}}}, \quad (3.27)$$

and

$$\mathcal{A} = L^{p-2} L_\xi (br_H^{-z}) \int_\epsilon^{r_t} dr \frac{1}{\sqrt{f}} \frac{r^{-\alpha_2}}{\sqrt{1 - (r/r_t)^{2\alpha_2}}}. \quad (3.28)$$

Note the extra dimensionless factor (br_H^{-z}) , which comes from the contribution $(1-f)b^2$ in front of $d\xi^2$ term. This factor gives us a chance that this entanglement entropy can be equal to the thermal entropy given in (3.18).

Assuming $\alpha_2 > 0$, we can rewrite the integrals as, following [77]

$$l = r_t \int_0^1 d\Omega \frac{\omega^{\alpha_2}}{\sqrt{1 - (\gamma\omega)^{2z} \sqrt{1 - \omega^{2\alpha_2}}}}, \quad (3.29)$$

and

$$\mathcal{A} = L^{d-1} L_\xi (br_H^{-z}) r_t^{1-\alpha_2} \int_{\epsilon/r_t}^1 d\Omega \left(\left[\frac{\omega^{-\alpha_2}}{\sqrt{1 - (\gamma\omega)^{2z} \sqrt{1 - \omega^{2\alpha_2}}}} - \frac{1}{\omega^{\alpha_2}} \right] + \frac{1}{\omega^{\alpha_2}} \right), \quad (3.30)$$

where the square bracket part is finite for $\alpha_2 > 0$ and

$$\omega = \frac{r}{r_t}, \quad \gamma = \frac{r_t}{r_H} < 1. \quad (3.31)$$

The last term can be computed as

$$\mathcal{A}_{div} = L^{p-2} L_\xi (br_H^{-z}) r_t^{1-\alpha_2} \int_{\epsilon/r_t}^1 d\Omega \frac{1}{\omega^{\alpha_2}} = L^{p-2} L_\xi (br_H^{-z}) \frac{1}{\alpha_2 - 1} \frac{1}{\epsilon^{\alpha_2 - 1}}, \quad (3.32)$$

which is the divergent contribution of the zero temperature background.

At small temperature, we can evaluate the integral as

$$l = r_t \int_0^1 d\Omega \frac{\omega^{\alpha_2}}{\sqrt{1 - (\gamma\omega)^{2z} \sqrt{1 - \omega^{2\alpha_2}}}} \approx \sqrt{\pi} r_t \frac{\Gamma\left(\frac{1+\alpha_2}{2\alpha_2}\right)}{\Gamma\left(\frac{1}{2\alpha_2}\right)} \quad (3.33)$$

and

$$\begin{aligned}\mathcal{A}_{fin} &\approx L^{p-2} L_\xi (br_H^{-z}) r_t^{1-\alpha_2} \int^1 d\Omega \frac{\omega^{-\alpha_2}}{\sqrt{1-\omega^{2\alpha_2}}} \left(1 + \frac{1}{2}(\gamma\omega)^{2z} + \dots \right), \\ &= L^{p-2} L_\xi (br_H^{-z}) l^{1-\alpha_2} c_\theta \left(-\frac{1}{\alpha_2-1} + \frac{\gamma^{2z}}{4\alpha_2} \frac{\Gamma\left(\frac{-\alpha_2+2z+1}{2\alpha_2}\right)}{\Gamma\left(\frac{2z+1}{2\alpha_2}\right)} \frac{\Gamma\left(\frac{1}{2\alpha_2}\right)}{\Gamma\left(\frac{1+\alpha_2}{2\alpha_2}\right)} + \dots \right),\end{aligned}\quad (3.34)$$

Thus, for the low temperature limit, the entanglement entropy for a strip in the general metric (3.22) is given in terms of (b, r_H) as

$$\begin{aligned}\mathcal{S} &= \frac{(RM_{Pl})^p}{4(\alpha_2-1)} \frac{b}{r_H^z} \left(\left(\frac{\epsilon}{R_\theta} \right)^\theta \frac{L^{p-2} L_\xi}{\epsilon^{p-z-1}} \right. \\ &\quad \left. - c_\theta \left(\frac{l}{R_\theta} \right)^\theta \frac{L^{p-2} L_\xi}{l^{p-z-1}} \left[1 - \tilde{c}_\theta \left(\frac{l}{r_H} \right)^{2z} + \dots \right] \right),\end{aligned}\quad (3.35)$$

where R_θ is a scale in which the hyperscaling violation becomes important and

$$c_\theta = \left(\frac{\sqrt{\pi} \Gamma\left(\frac{1+\alpha_2}{2\alpha_2}\right)}{\Gamma\left(\frac{1}{2\alpha_2}\right)} \right)^{\alpha_2}, \quad \tilde{c}_\theta = \frac{(\alpha_2-1)\sqrt{\pi}}{4\alpha_2} c_\theta^{-\frac{2z+1}{\alpha_2}} \frac{\Gamma\left(\frac{-\alpha_2+2z+1}{2\alpha_2}\right)}{\Gamma\left(\frac{2z+1}{2\alpha_2}\right)}.\quad (3.36)$$

Note that the scaling mismatches of the factor $\frac{L^{p-2} L_\xi}{\epsilon^{p-z-1}}$ and $\frac{L^{p-2} L_\xi}{l^{p-z-1}}$ are made up by that of $\frac{b}{r_H^z}$.

In the high temperature limit,

$$l = r_t \int^1 d\Omega \frac{\omega^{\alpha_2}}{\sqrt{1-(\gamma\omega)^{2z}} \sqrt{1-\omega^{2\alpha_2}}} = r_t I_+(\gamma),\quad (3.37)$$

and

$$\begin{aligned}\mathcal{A} &= L^{p-2} L_\xi (br_H^{-z}) r_t^{1-\alpha_2} \int^1 d\Omega \frac{\omega^{-\alpha_2}}{\sqrt{1-(\gamma\omega)^{2z}} \sqrt{1-\omega^{2\alpha_2}}} \\ &= L^{p-2} L_\xi (br_H^{-z}) r_t^{1-\alpha_2} I_-(\gamma).\end{aligned}\quad (3.38)$$

When $\gamma \rightarrow 1, r_t \approx r_H$, the integrals $I_+(\gamma)$ and $I_-(\gamma)$ are dominated by the contribution $\omega \approx 1$ and thus $I_+(\gamma) \approx I_-(\gamma) \approx l/r_t$ [8]. Thus

$$\mathcal{S}_{fin} \approx \frac{(M_{pl}R)^p}{4} R_\theta^{-\theta} L^{p-2} L_\xi l b r_H^{-p+\theta} = \frac{(M_{pl}R)^p}{4} R_\theta^{-\theta} L^{p-2} L_\xi l b r_H^{-\frac{9-p}{5-p}},\quad (3.39)$$

which agrees with the thermal entropy evaluated in (3.18).

3.3 Searching for effective theories

In this section, we would like to answer a question, “*Can we construct the most general low energy and lower dimensional effective holographic metrics with Schrödinger scaling at finite temperature?*” The answer seems to be partial due to the special form we consider.

For now, we can think about the class of metrics of the form with two parameters (θ, z)

$$ds^2 = r^{\frac{2\theta}{p}-2} K^{\frac{1}{p}} \left[\frac{-f dt^2}{(1-f)b^2} + \frac{(1-f)b^2}{K} \left(d\xi - \frac{1+f}{1-f} \frac{dt}{2b^2} \right)^2 + \sum_{i=1}^{p-1} dx_i^2 + \frac{dr^2}{f} \right],$$

$$f = 1 - \left(\frac{r}{r_H} \right)^{2z}, \quad K = 1 + \beta b^2 r_H^{-2z} r^2. \quad (3.40)$$

Note the emblackening factor f , whose form is fixed only with dynamical exponent z . Let us comment the scaling symmetry of the metric (3.7), which is described by the transformations

$$t \rightarrow \lambda^z t, \quad \xi \rightarrow \lambda^{2-z} \xi, \quad r \rightarrow \lambda r, \quad x_i \rightarrow \lambda x_i, \quad (3.41)$$

$$b \rightarrow \lambda^{z-1} b, \quad \beta \rightarrow \lambda^0 \beta, \quad r_H \rightarrow \lambda r_H. \quad (3.42)$$

The corresponding zero temperature limit is explicitly considered in §3.1.1. We would like to investigate the physical properties of this metric from the spirit of §2.1 for $z > 0$ and postpone an important question whether this class of metrics can be further generalized.

Can we restrict further the allowed regions of the parameter space of (θ, z) using specific heat constraint? We already calculate them in (3.18) of §3.1.2.

$$T \sim \frac{1}{br_H}, \quad S_T \sim br_H^{-p+\theta}, \quad \Omega = \frac{1}{2b^2}. \quad (3.43)$$

From these thermodynamic quantities, we calculate the specific heat for fixed Ω for $z > 0$, even though the result is less restrictive than that for fixed particle number N .¹² The condition $T \frac{\partial S}{\partial T} |_{\Omega} > 0$ gives $\theta < p = d + 1$ for $z > 0$. This condition is actually less restrictive than the entanglement entropy constraint, $\theta < d + 2 - z$. Thus we are not able to constrain more than what we did with the zero temperature metric once we include the constraint entanglement entropy analysis as well as null energy conditions, which are analyzed in [11]. In particular, the null energy condition gives two independent constraints

$$(z-1)(d+2z)(d+1) - z(d+1)\theta + \theta^2 \geq 0,$$

$$(z-1)(d+2z-\theta) \geq 0, \quad (3.44)$$

¹² It is expected to constrain the parameter space more strictly if we use the specific heat with fixed particle number. The over all sign of the ΩN term is negative similar to the pressure and volume PV , where C_V is more constraining than C_P at least for the ideal thermodynamics. It would be interesting to evaluate all the thermodynamic quantities including energy E and dual particle number N . Simply these are not available yet. Thus we would like to consider a specific heat with fixed Ω to constrain the parameter spaces. We thanks to Carlos Hoyos for the discussions related to this point.

where we use $D = p = d + 1$.

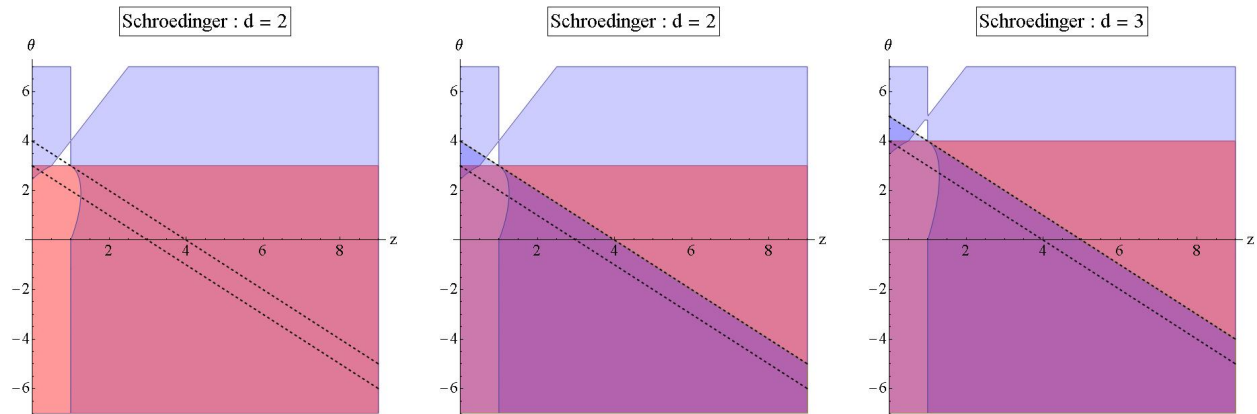


Figure 3: The left plot shows the allowed region (dark red) for the Schrödinger background for $d = 2$ after taking into account of the specific heat condition for fixed Ω , $\theta < d + 1$ in addition to the null energy condition. The region between two dashed lines indicates some novel phases from the entanglement entropy analysis [11]. The left plot can be further constrained by the entanglement entropy analysis, $\theta < d + 2 - z$, which is given in the middle plot. Thus the purple region is allowed for $z > 0$. The right plot shows the regions allowed by the null energy condition (blue), the specific heat (red), and the entanglement analysis. The purple region is allowed after taking into account these conditions for $d = 3$.

Can we remove the parameter b for the low energy description? The answer is no. The reason is already stressed above that the physical parameter b has a crucial role in black hole thermodynamics. Thus any change would result in changing its thermodynamics, which is not allowed. Furthermore, b is relevant for all energy scales because it has zero mass dimension, while it carries definite scaling dimensions.

Let us finish this section by commenting the case $z < 0$. Seeming there are several different solutions with *negative* dynamical exponents, which can be obtained from the consistent string theory backgrounds [97][113][114].¹³ While it is not clear that these theories are consistent or useful, it is interesting to have careful investigations for them. Some holographic backgrounds with negative dynamical exponents are also reported in different contexts, see *e.g.* [12]. We also find that the null Melvin twisted version of the seemingly non-singular KK monopole solution exhibits a negative dynamical exponent §B.5.

4 Theories with Schrödinger scaling II

As we already point out, there are two different realizations of holographic theories with Schrödinger scaling. Here we consider a simpler realization, so-called AdS in light-cone

¹³We thank to Nikolay Bobev and especially Yaron Oz for the references and related discussions and comments.

(ALCF). The case without hyperscaling violation, $\theta = 0$, is introduced in [115][116], and further generalized to finite temperature in [84][112]. The transport properties of this background is analyzed in [112][117]. The magneto-transport properties analyzed in [117] are very similar to those of the high T_c cuprates at very low temperature. See also [118]. The transport properties are further generalized using higher derivative corrections in [119].

At zero temperature, ALCF are described by the metric (1.1) with $b = 0, a = 1$

$$ds^2 = r^{-2+\frac{2\theta}{d+1}} \left(-2 dt d\xi + dr^2 + \sum_{i=1}^c dx_i^2 + \sum_{j=c+1}^d \eta_j(r, t, \vec{x}) dx_j^2 \right), \quad (4.1)$$

where $D = d+1$. This metric is also analyzed in [11] along with the Schrödinger backgrounds (3.2) for both cases with and without hyperscaling violation exponent. There similar results on the minimal surface prescriptions and thus entanglement entropy are obtained. Recently, hyperscaling violation of the R-charged black holes are analyzed in [30].

The program to restrict the parameter space of (z, θ) of the metric (4.1) for d spatial dimensions is carried out with the null energy condition, which are depicted in figure 3 for $d = 2$ and 3 [11]. For this case, the null energy condition is similar to the Lifshitz case, while the entanglement entropy condition is similar to Schrödinger backgrounds with non-trivial dependence on z . Thus the classification at zero temperature works as the other cases.

The program of classifying ALCF at finite temperature has the similar difficulties as the Schrödinger background. See the introduction of §3. Thus we concentrate on the ALCF version of the relativistic black Dp branes solutions as our prime examples and dimensionally reduce them to understand their physical properties in §4.1. We find the dynamical exponent of the ALCF at finite temperature is not fixed by the parameters of the microscopic string theories. In the rest of §4.1, we study the thermodynamics ALCF and their dimensional reduction to Lifshitz theories along the ξ coordinate. We study the finite temperature entanglement entropy in §3.2, followed by the effective approach based on the results of the dimensional reduction in §3.3.

4.1 String theory realizations for ALCF

We are primarily interested in the black Dp branes solutions [110][111][37], whose metric is given by

$$ds_{Dp}^2 = h^{-1/2} \left(-f d\tau^2 + \sum_{i=1}^p dx_i^2 \right) + \frac{h^{1/2}}{\tilde{r}^4} \left(\frac{1}{f} d\tilde{r}^2 + \tilde{r}^2 d\Omega_{8-p}^2 \right), \quad (4.2)$$

$$f = 1 - \left(\frac{\tilde{r}}{\tilde{r}_H} \right)^{7-p}, \quad h = 1 + \left(\frac{\tilde{r}}{\tilde{r}_0} \right)^{7-p}, \quad e^{-2(\Phi - \Phi_\infty)} = h^{(p-3)/2}, \quad (4.3)$$

where we omit RR fields and the corresponding type II supergravity action. We compactify this solution on S^{8-p} down to $(p+2)$ dimensions to get

$$ds_{p+2}^2 = h^{-1/2} \left(-f d\tau^2 + \sum_{i=1}^p dx_i^2 \right) + \frac{h^{1/2}}{\tilde{r}^4 f} d\tilde{r}^2, \quad (4.4)$$

and the action acquire additional radial dependence from the radial dependence of S^{8-p}

$$S = \frac{V(\Omega_{8-p})}{2\kappa_{10}^2} \int d^{p+2}x \sqrt{-g_{p+2}} e^{-2\Phi_{p+2}} \mathcal{R}_{p+2} + \dots, \quad (4.5)$$

where $e^{-2\Phi_{p+2}} = h^{\frac{p+2}{4}} \tilde{r}^{p-8}$ represents the radial dependence, not a dilaton. Using $ds^2 \rightarrow (e^{-2\Phi_{p+2}})^{\frac{2}{p}} ds^2$, we go to the Einstein frame in $p+2$ dimensions

$$ds_{Dp}^2 = r^{-\frac{2(9-p)}{p(5-p)}} \left(-f d\tau^2 + \sum_{i=1}^p dx_i^2 + \frac{1}{f} dr^2 \right), \quad f = 1 - \left(\frac{r}{r_H} \right)^{\frac{2(7-p)}{5-p}}, \quad (4.6)$$

where we use $h \rightarrow \left(\frac{\tilde{r}}{\tilde{r}_0} \right)^{7-p}$ for the near horizon limit and additional change of a variable $\tilde{r} \sim r^{\frac{2}{5-p}}$. The overall dimensionful factor was not carried over.

The operation of the dimensional reduction commutes with changing into the light-cone frame, which is defined by

$$t = b(\tau + x), \quad \xi = \frac{1}{2b}(\tau - x). \quad (4.7)$$

We assign the scaling dimension of b as $[b] = 1 - z$ in the mass unit, and thus $[t] = -z$ and $[\xi] = z - 2$ to have manifest dynamical exponent z . The metric takes the form

$$ds^2 = r^{-\frac{2(9-p)}{p(5-p)}} \left(\frac{1-f}{4b^2} dt^2 - (1+f) dt d\xi + (1-f)b^2 d\xi^2 + \sum_{i=1}^{p-1} dx_i^2 + \frac{1}{f} dr^2 \right). \quad (4.8)$$

At zero temperature, $f = 1$, this metric is reduced to

$$ds^2 = r^{-\frac{2(9-p)}{p(5-p)}} \left(-2 dt d\xi + \sum_{i=1}^{p-1} dx_i^2 + dr^2 \right). \quad (4.9)$$

The basic properties of this metric was analyzed in [11]. We have the following identification for θ

$$\theta_{LC} = -\frac{(p-3)^2}{5-p}, \quad (4.10)$$

where we use $D = p = d + 1$ for the Schrödinger case.

For later use, we would like to explicitly write the physical ADM form

$$ds^2 = \left(\frac{r}{R_\theta} \right)^{-\frac{2(9-p)}{p(5-p)}} \left(\frac{-f dt^2}{(1-f)b^2} + (1-f)b^2 \left(d\xi - \frac{1+f}{1-f} \frac{dt}{2b^2} \right)^2 + \sum_{i=1}^{p-1} dx_i^2 + \frac{dr^2}{f} \right), \quad (4.11)$$

where R_θ represent a scale where the hyperscaling violation becomes significant. Let us comment the scaling symmetry of the metric (4.11), which is described by the transformations

$$t \rightarrow \lambda^z t, \quad \xi \rightarrow \lambda^{2-z} \xi, \quad r \rightarrow \lambda r, \quad x_i \rightarrow \lambda x_i, \quad b \rightarrow \lambda^{z-1} b, \quad r_H \rightarrow \lambda r_H. \quad (4.12)$$

Similar to the Schrödinger background, we would like to determine the dynamical exponent for the ALCF metric (4.11). We would like to remind the reader that the identification of the dynamical exponent z is not clear for the zero temperature metric (4.9). Actually the metric (4.9) describes ALCF system for general z at zero temperature [11]. Furthermore, the scaling transformation (4.12) does not fix the dynamical exponent in terms of other parameters, such as p . Thus we leave the dynamical exponent undetermined for the case here, too.¹⁴

4.1.1 Thermodynamic Properties

Thermodynamic properties of the metric (4.8) are more transparent in the ADM form (4.11). From this ADM form, we can read off the lapse function N , the shift function V^i and the horizon coordinate velocity in the x^- direction Ω_H , which can be interpreted as chemical potential associated with the conserved quantities along the x^- direction, as

$$N = r^{-\frac{9-p}{p(5-p)}} \sqrt{\frac{f}{(1-f)b^2}}, \quad V^- = -\frac{1}{2b^2} \frac{1+f}{1-f}, \quad \Omega_H = \frac{1}{2b^2}. \quad (4.13)$$

Some of the thermodynamic properties can be directly analyzed using the horizon properties. The temperature, entropy and chemical potential along the ξ direction are given by

$$T = \frac{1}{2\pi b r_H} \left| \frac{7-p}{5-p} \right|, \quad S_T = b \left(\frac{r_H}{R_\theta} \right)^{-\frac{9-p}{5-p}} V_{p-1} V_\xi, \quad \Omega = \frac{1}{2b^2}. \quad (4.14)$$

Due to the presence of the parameter b , it is not straightforward to identify the precise relation between the thermal entropy S_T and the temperature T .

¹⁴ From this metric (4.11), we consider the first term in the parenthesis $\frac{-f}{(1-f)b^2} = -b^{-2} r_H^{\frac{2(7-p)}{5-p}} r^{-\frac{2(7-p)}{5-p}} f$ where the dimensionful parameters $b^{-2} r_H^{\frac{2(7-p)}{5-p}}$ can be absorbed by redefining the coordinate t . It is tempting to identify the dynamical exponent z_{LC} as $z_{LC} = 1 + \frac{7-p}{5-p} = \frac{12-2p}{5-p}$. But this is dangerous thing to do due to the fact that physical thermodynamic parameters are absorbed in time.

4.1.2 Reduction to theories with Lifshitz scaling

As done in the Schrödinger type theories, here we just formally identify the exponents of the ALCF theories to that of the Lifshitz theories by dimensionally reducing (4.11) along ξ coordinate.

The resulting $p+1$ dimensional Lifshitz type solution has the following metric in Einstein frame

$$ds^2 = r^{-\frac{4}{(p-1)(5-p)}} \left[-f r^{-\frac{2(7-p)}{5-p}} dt^2 + \sum_{i=1}^{p-1} dx_i^2 + \frac{dr^2}{f} \right], \quad (4.15)$$

where we also take $br_H^{-\frac{7-p}{5-p}} = 1$ as we comment in footnote 11. Now the metric has the same emblackening factor $f = 1 - \left(\frac{r}{r_H}\right)^{\frac{2(7-p)}{5-p}}$ as that of (3.19) considered in §3.1.3. We note that this form is the same as that of the Schrödinger case. Thus we identify

$$\theta_{LF} = -\frac{p^2 - 6p + 7}{5 - p}, \quad z_{LF} = \frac{12 - 2p}{5 - p}. \quad (4.16)$$

We would like to emphasize that this case also belongs to the typical case of emblackening factor, which can be identified as

$$d + z_{LF} - \theta_{LF} = \frac{2(7-p)}{5-p}, \quad f = 1 - \left(\frac{r}{r_H}\right)^{d+z_{LF}-\theta_{LF}}, \quad (4.17)$$

which seems to be persisting for this case also, as advertised in §2.1.

4.2 Entanglement entropy

We would like to evaluate the entanglement entropy for the ALCF background at finite temperature described by the metric (4.11) following [77][8].

$$ds^2 = \left(\frac{r}{R_\theta}\right)^{-2+2\theta/p} \left[\frac{-f dt^2}{(1-f)b^2} + (1-f)b^2 \left(d\xi - \frac{1+f}{1-f} \frac{dt}{2b^2} \right)^2 + \sum_{i=1}^{p-1} dx_i^2 + \frac{dr^2}{f} \right],$$

$$f = 1 - \left(\frac{r}{r_H}\right)^{\frac{2(7-p)}{5-p}}, \quad (4.18)$$

where $D = p = d + 1$. Note that we did not specify the emblackening factor in terms of z .

The entanglement entropy of the metric (4.18) with finite temperature can be computed for a strip with ξ direction

$$0 \leq \xi \leq L_\xi, \quad -l \leq x_1 \leq l, \quad 0 \leq x_i \leq L, \quad i = 2, \dots, p-1 \quad (4.19)$$

in the limit $l \ll L, L_\xi$. The strip is located at $r = \epsilon$, and the profile of the surface in the bulk is given by $r = r(x_1)$. The minimal surface has turning point at $r = r_t$. Thus, to get the entanglement entropy, we evaluate the following expressions

$$l = \int_0^{r_t} dr \frac{1}{\sqrt{f}} \frac{(r/r_t)^{\alpha_2}}{\sqrt{1 - (r/r_t)^{2\alpha_2}}} , \quad (4.20)$$

and

$$\mathcal{A} = L^{p-2} L_\xi \left(br_H^{-\frac{7-p}{5-p}} \right) \int_\epsilon^{r_t} dr \frac{1}{\sqrt{f}} \frac{r^{-\alpha_2}}{\sqrt{1 - (r/r_t)^{2\alpha_2}}} , \quad (4.21)$$

where $\alpha_2 = p - \frac{7-p}{5-p} - \theta$. Note that there is a clear difference compared to (2.6), the extra dimensionless factor $\left(br_H^{-\frac{7-p}{5-p}} \right)$, which comes from the contribution $(1-f)b^2$ in front of $d\xi^2$ term. This factor gives us a chance that this entanglement entropy can be equal to the thermal entropy (4.14).

The rest of the calculations are similar to the previous case §3.2, and we present the final results. For the low temperature limit, the entanglement entropy for a strip in the general metric (4.18) is given by

$$\mathcal{S} = \frac{(RM_{Pl})^p}{4(\alpha_2 - 1)} \frac{b}{r_H^{\frac{7-p}{5-p}}} \left(\left(\frac{\epsilon}{R_\theta} \right)^\theta \frac{L^{p-2} L_\xi}{\epsilon^{p-1-\frac{7-p}{5-p}}} - c_\theta \left(\frac{l}{R_\theta} \right)^\theta \frac{L^{p-2} L_\xi}{l^{p-1-\frac{7-p}{5-p}}} \left[1 - \tilde{c}_\theta \left(\frac{l}{r_H} \right)^{2\frac{7-p}{5-p}} + \dots \right] \right) , \quad (4.22)$$

which has the same form as (3.35) with suitable identification of z , which we do not specify due to the reason explained above.

In the high temperature limit,

$$l = r_t \int^1 d\Omega \frac{\omega^{\alpha_2}}{\sqrt{1 - (\gamma\omega)^{2z-2}} \sqrt{1 - \omega^{2\alpha_2}}} = r_t I_+(\gamma) , \quad (4.23)$$

and

$$\begin{aligned} \mathcal{A} &= L^{d-1} L_\xi \left(br_H^{-\frac{7-p}{5-p}} \right) r_t^{1-\alpha_2} \int^1 d\Omega \frac{\omega^{-\alpha_2}}{\sqrt{1 - (\gamma\omega)^{2z-2}} \sqrt{1 - \omega^{2\alpha_2}}} \\ &= L^{d-1} L_\xi \left(br_H^{-\frac{7-p}{5-p}} \right) r_t^{1-\alpha_2} I_-(\gamma) . \end{aligned} \quad (4.24)$$

When $\gamma \rightarrow 1, r_t \approx r_H$, the integrals $I_+(\gamma)$ and $I_-(\gamma)$ are dominated by the contribution $\omega \approx 1$ and thus $I_+(\gamma) \approx I_-(\gamma) \approx l/r_t$ [8]. Thus

$$\mathcal{S}_{fin} \approx R_\theta^{-\theta} L^{d-1} L_\xi l b r_H^{-p+\theta} = R_\theta^{-\theta} L^{d-1} L_\xi l b r_H^{-\frac{9-p}{5-p}} , \quad (4.25)$$

which agrees with the thermal entropy evaluated in (4.14).

4.3 Searching for ALCF effective theories

In this section, we would like to ask a similar question, “*Can we construct the most general low energy and lower dimensional ALCF effective holographic metrics with Schrödinger scaling at finite temperature?*” The answer seems to be more unclear for this case compared to Schrödinger case at finite temperature.

For now, we can think about the class of metrics of the form with a parameter θ for arbitrary z

$$ds^2 = r^{\frac{2\theta}{p}-2} \left[\frac{-f dt^2}{(1-f)b^2} + (1-f)b^2 \left(d\xi - \frac{1+f}{1-f} \frac{dt}{2b^2} \right)^2 + \sum_{i=1}^{p-1} dx_i^2 + \frac{dr^2}{f} \right],$$

$$f = 1 - \left(\frac{r}{r_H} \right)^{\frac{7-p}{5-p}}. \quad (4.26)$$

Note the emblackening factor f does not have a definite dependence on z , due to the fact that this metric is valid for arbitrary dynamical exponent z [11]. See also the discussion around (4.11). With this form, specific heat constraint from (4.14) does not give us further constraint because the expressions are well defined for given p .

Now we change our attention a little and try to understand the differences between the Schrödinger backgrounds (3.40) and those of ALCF (4.26). For this purpose we fix the dynamical exponent of the ALCF metric as $z_{LC} = \frac{7-p}{5-p}$. Thus for the rest of the section we consider the metric

$$ds^2 = r^{\frac{2\theta}{p}-2} \left[\frac{-f dt^2}{(1-f)b^2} + (1-f)b^2 \left(d\xi - \frac{1+f}{1-f} \frac{dt}{2b^2} \right)^2 + \sum_{i=1}^{p-1} dx_i^2 + \frac{dr^2}{f} \right],$$

$$f = 1 - \left(\frac{r}{r_H} \right)^z. \quad (4.27)$$

Thermodynamical properties of this metric is given by

$$T \sim \frac{1}{br_H}, \quad S_T \sim br_H^{\theta-p}, \quad \Omega = \frac{1}{2b^2}. \quad (4.28)$$

Similar to the discussion around the equation (3.43) and footnote 12, we would like to restrict further the allowed regions of the parameter space of (θ, z) using specific heat constraint at fixed Ω . The condition $T \frac{\partial S}{\partial T} |_{\Omega} > 0$ gives $\theta < p = d + 1$ for $z > 0$. This condition is actually less restrictive than the entanglement entropy constraint, $\theta < d + 2 - z$, which might be improved once we can use the specific heat constraint for fixed particle number.

Thus we have the following constraints. At zero temperature, we have the entanglement entropy analysis $\theta < d + 2 - z$ as well as the null energy conditions [11].

$$\theta(\theta - d - 1) \geq 0 \quad \rightarrow \quad \theta \leq 0 \quad \text{or} \quad \theta \geq d + 1. \quad (4.29)$$

At finite temperature, we add $\theta < p = d + 1$ for $z > 0$ from specific heat constraint at fixed chemical potential Ω . This is summarized in figure 4.

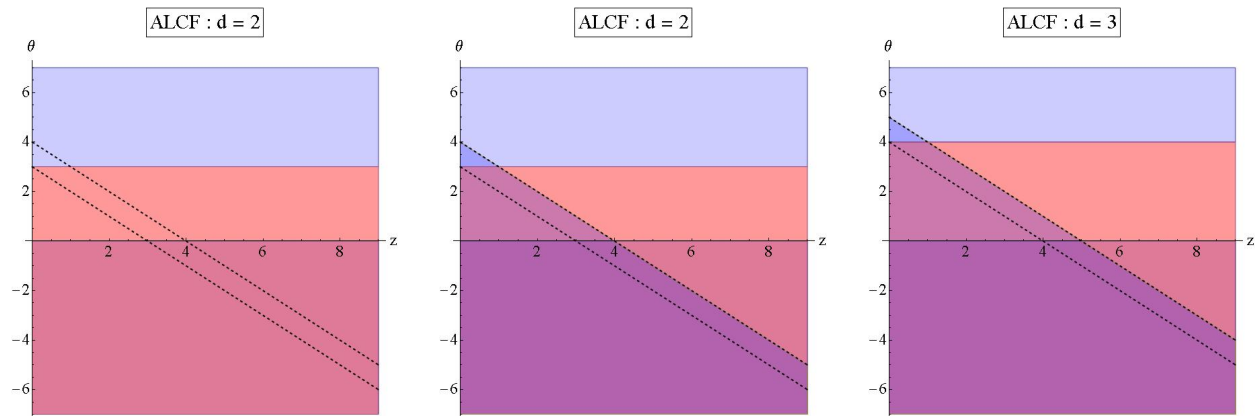


Figure 4: The left plot shows the allowed region (dark red) for the Schrödinger background for $d = 2$ after taking into account of the specific heat condition for fixed Ω , $\theta < d + 1$ in addition to the null energy condition. The region between two dashed lines indicates some novel phases from the entanglement entropy analysis [11]. The left plot can be further constrained by the entanglement entropy analysis, $\theta < d + 2 - z$, which is given in the middle plot. Thus the purple region is allowed for $z > 0$. The right plot shows the regions allowed by the null energy condition (blue), the specific heat (red), and the entanglement analysis. The purple region is allowed after taking into account these conditions for $d = 3$.

5 Summary and Outlook

The main theme we would like to put forward is that *the hyperscaling violation exponent θ along with the dynamical z and the spatial anisotropic \ddagger exponents can be viewed a unified framework for the low energy and lower dimensional effective holographic theories*. One clear observation is that the hyperscaling violation exponent captures the degree of violation of conformal symmetry of the microscopic string theory solutions. Conformal invariant solutions would give $\theta = 0$ upon simple dimensional reduction, while nonconformal solutions would produce non zero θ .

We initiate a simple classification of these effective holographic theories with definite scaling symmetries. Our examples include the theories with Lifshitz, including the relativistic $z = 1$ case, and Schrödinger scaling. Our classification is simple because we only care about the metric, discarding the corresponding action and matter contents. This can be justified, partially at least, by the fact that one metric can be supported by more than single set of action with corresponding matter contents [50]. Thus classifying theories with full solutions might be redundant, certainly for the physical properties directly related to the metric.

As shown in the main body, this program is successful for the theories with Lifshitz scaling, which is described by the simple metric (2.1)

$$ds_{d+2}^2 = r^{-2(d-\theta)/d} \left(-r^{-2(z-1)} f(r) dt^2 + \frac{dr^2}{f(r)} + \sum_{i=1}^d dx_i^2 \right),$$

$$f(r) = 1 - \left(\frac{r}{r_H} \right)^{d+z-\theta}, \quad (5.1)$$

where θ and z are the hyperscaling violation and dynamical exponents. This metric is extensively studied in the context of Einstein-Maxwell system with a dilaton [4][71] and in the context of systems with hyperscaling violation [7][8]. Several observations are in order. First, many different microscopic string solutions reduce to this simple and universal form upon sphere reduction, as we have checked here. The metric is universal even at finite temperature with a fixed emblackening factor f . Second, the information of the dimensionful parameter in the string theory solution is directly transferred to the front factor, captured by the hyperscaling violation exponent θ . Third, this metric has been known to be the most general IR scaling solution for Einstein-Maxwell system with one scalar [5]. Fourth, if there are more than one dimensionful parameters active in the effective theories, additional exponents, called spatial anisotropic exponents, would come into play.

Once one accepts this, further procedures are required to restrict the allowed space of the parameters (z, θ) [6][8]. This can be done by using null energy conditions and the condition from entanglement entropy analysis at zero temperature. The allowed parameter space is further restricted by the positive specific heat constraint. The result for the theories with Lifshitz scaling is summarized in the figure 1. This result is tested against the earlier, similar in spirit, program to constrain the allowed parameter space of the full solution [4][51], using the Gubser's constraint [75] as well as the well defined fluctuation problems around the horizon. The allowed regions of the latter is summarized in the figure 2. After taking into account of the positive specific heat constraint, these two programs to restrict the allowed region of the parameter space (z, θ) are identical, signalling success of our program at least for the theories with Lifshitz isometry.

We also consider two different theories with Schrödinger scaling : Schrödinger backgrounds and ALCF (AdS in light-cone). The classification goes well at zero temperature similar to that of the Lifshitz isometry.

$$ds^2 = r^{-2+2\theta/D} \left(-b r^{2-2z} dt^2 - 2dt d\xi + dr^2 + \sum_{i=1}^c dx_i^2 + \sum_{j=c+1}^d r^{2-2\sharp_j} dx_j^2 \right), \quad (5.2)$$

where $D = d + 1$ and \sharp_j are the spatial anisotropic exponents. We consider here two different theories, Schrödinger backgrounds with $b = 1$ and ALCF with $b = 0$. At finite temperature,

there exist additional dimensionful parameter b entering our story, which also has role in their thermodynamics. We can not simply remove or absorb this b without changing their physical properties. Thus we should carry over this parameter. The classification becomes complicated in the description of the effective theories because there are many different scaling invariant combinations one can come up with the parameter b along with the radial direction and other parameters in the theory. Thus the program need much more care compared to that of the Lifshitz case. The results are summarized in the figure 3 for the Schrödinger case and in the figure 4 for the ALCF.

We are observing intricate and active interplay between many different disciplines, especially the string theory and condensed matter, via gauge gravity duality. Our program would be useful for the high energy community to provide useful guides for the available theories with various scaling symmetries, not to mention for the condense matter applications. We investigate the systematic studies of the holographic backgrounds with scaling symmetries using the simplest sphere reduction. It is interesting to generalize this program by incorporating non-trivial internal geometries and various higher modes in the dimensional reduction as well as by tackling less symmetric holographic backgrounds. Generally, it is expected to introduce more exponents as the reduction becomes more complicated. Theories with Schrödinger isometry are more involved due to the presence of a new thermodynamic parameter at finite temperature and requires more investigations. It will be also interesting to investigate further the backgrounds with the negative dynamical exponents.

Acknowledgments

We are grateful to N. Bobev, C. Charmousis, O. Ganor, B. Goutéraux, C. Hoyos, S. Hyun, N. Itzhaki, J. Jeong, E. Kiritsis, B.-H. Lee, R. Meyer, K. Narayan, Y. Oz, Y. Seo, S.-J. Sin, C. Sonnenschein and P.-j. Yi for discussions, correspondences and comments. We are indebted to Yaron Oz for the collaboration at the early stage and for valuable comments on the draft. Various parts of the paper have been developed through his numerous advices. We thank to the members of the CQUeST for their warm hospitality and to the organizers of “APCTP Focus Program : Holography at LHC,” Aug. 1-10, 2012 at APCTP, Pohang, Korea. Some of the results were presented there, and the author received valuable comments. We are supported in part by the Centre of Excellence supported by the Israel Science Foundation (grant number 1468/06).

Appendix

A Dimensional reduction of theories with Lifshitz scaling

In this section, we consider several different string theory solutions and their dimensional reductions (simple sphere reduction) of their compact coordinates. We compare the resulting backgrounds to the general form given in (1.1) to check whether we can get some useful information, which is universal over several different examples. In particular, all the worked out examples in this section has the metric structure given in (2.1) at finite temperature (if the finite temperature generalizations are available). For the convenience, we write the metric here again

$$ds_{d+2}^2 = r^{-2(d-\theta)/d} \left(-r^{-2(z-1)} f(r) dt^2 + \frac{dr^2}{f(r)} + \sum_{i=1}^d dx_i^2 \right), \quad f(r) = 1 - \left(\frac{r}{r_H} \right)^{d+z-\theta}.$$

The examples we consider here include the Dp branes, M2, M5 branes, Dp-Dq and intersecting M-brane systems.

A.1 Near extremal Black Dp branes

Dimension reduction of Dp branes in the context of hyperscaling violation are analyzed in [8]. This serves as our prime examples. Here we add some more details. The 10 dimensional non-extremal Dp brane metric in string frame is

$$\begin{aligned} ds_{Dp, str}^2 &= H^{-1/2} \left(-f dt^2 + \sum_{i=1}^p dx_i^2 \right) + H^{1/2} \left(\frac{d\tilde{r}^2}{f} + \tilde{r}^2 d\Omega_{8-p}^2 \right), \quad (\text{A.1}) \\ H &= 1 + \sinh^2 \beta \frac{\tilde{r}_H^{7-p}}{\tilde{r}^{7-p}}, \quad f = 1 - \frac{\tilde{r}_H^{7-p}}{\tilde{r}^{7-p}}, \\ e^{\phi-\phi_0} &= g_s H^{(3-p)/4}, \quad C_{01\dots p} = \coth \beta g_s^{-1} (1 - H^{-1}). \end{aligned}$$

To analyze the thermodynamic properties and dimensional reduction later, we rewrite the metric in Einstein frame using $ds_E^2 = e^{-\phi/2} ds_{str}^2 = H^{\frac{p-3}{8}} ds_{str}^2$.

$$ds_{Dp, E}^2 = H^{-(7-p)/8} \left(-f dt^2 + \sum_{i=1}^p dx_i^2 \right) + H^{(p+1)/8} \left(\frac{d\tilde{r}^2}{f} + \tilde{r}^2 d\Omega_{8-p}^2 \right). \quad (\text{A.2})$$

The temperature and entropy of the geometry are given by

$$T = \frac{7-p}{4\pi \cosh \beta \tilde{r}_H}, \quad S = \frac{\Omega_{8-p}}{4G_{10}} V_p \cosh \beta \tilde{r}_H^{8-p}, \quad (\text{A.3})$$

where Ω_{8-p} is the volume of the S^{8-p} , and we use $H = 1 + \sinh^2 \beta \frac{\tilde{r}_H^{7-p}}{\tilde{r}^{7-p}} = \cosh^2 \beta$.

We also consider the near extremal limit for a small temperature, $H = 1 + \sinh^2 \beta \frac{\tilde{r}_0^{7-p}}{\tilde{r}^{7-p}} \rightarrow \frac{\tilde{r}_0^{7-p}}{\tilde{r}^{7-p}}$. The temperature and entropy of the geometry for the near extremal limit are given by

$$T = \frac{f'(\tilde{r}_H)}{4\pi H(\tilde{r}_H)^{1/2}} = \frac{7-p}{4\pi} \frac{\tilde{r}_H^{(5-p)/2}}{\tilde{r}_0^{(7-p)/2}}, \quad (\text{A.4})$$

$$S = \frac{V_p V(S^{8-p})}{4G_{10}} H(\tilde{r}_H)^{1/2} \tilde{r}_H^{8-p} = \frac{\Omega_{8-p} V_p \tilde{r}_0^{(7-p)/2} \tilde{r}_H^{(9-p)/2}}{4G_{10}}, \quad (\text{A.5})$$

where we use the volume of unit n sphere (surface area of unit $n+1$ dimensional ball) $\Omega_n = \frac{2\pi^{(n+1)/2}}{\Gamma((n+1)/2)}$. Thus we check the temperature dependence of the entropy $S \sim T^{\frac{9-p}{5-p}}$ in the near extremal limit.

With these basic information, we would like to compactify this theory on S^{8-p} down to $p+2$ dimensions. Here the action has the form

$$\begin{aligned} S &= \frac{1}{2\kappa_{10}^2} \int d^{10}x \sqrt{-g} \mathcal{R} + \dots \\ &= \frac{V(S^{8-p}) R^{8-p}}{2\kappa_{10}^2} \int d^{p+2}x \sqrt{-g_{p+2}} e^{-2\Phi_{p+2}} (\mathcal{R}_{p+2} + \dots), \end{aligned} \quad (\text{A.6})$$

where R is some dimensionful constant to match the dimension. Here it is natural to take $R = \tilde{r}_0$. In the main body, we assume that there is a dimensionful parameter to match the dimension after the dimensional reduction. $e^{-2\Phi_{p+2}}$ represents \tilde{r} dependence coming from the compactification, and the lower dimensional newton constant κ_{p+2} can be expressed explicitly. They are

$$e^{-2\Phi_{p+2}} = H^{(p+1)(8-p)/16} \left(\frac{\tilde{r}}{R} \right)^{8-p}, \quad \frac{1}{2\kappa_{p+2}^2} = \frac{V(S^{8-p}) R^{8-p}}{2\kappa_{10}^2}. \quad (\text{A.7})$$

Note that Φ_{p+2} is not a dilaton. Finally, using $ds^2 \rightarrow (e^{-2\Phi_{p+2}})^{\frac{2}{p}} ds^2$, the Einstein frame metric has the following form

$$ds_{p,E}^2 = H^{\frac{1}{p}} \left(\frac{\tilde{r}}{R} \right)^{\frac{2(8-p)}{p}} \left(-f dt^2 + \sum_{i=1}^p dx_i^2 + H \frac{d\tilde{r}^2}{f} \right), \quad (\text{A.8})$$

By changing a variable $H^{1/2} d\tilde{r} = dr$, we can get the standard form.

We explicitly consider the near extremal limit, $H \approx \frac{\tilde{r}_0^{7-p}}{\tilde{r}^{7-p}}$. Then we get

$$ds_{p,E}^2 = \left(\frac{\tilde{r}_0^{7-p}}{\tilde{r}^{7-p}} \right)^{\frac{1}{p}} \left(\frac{\tilde{r}}{R} \right)^{\frac{2(8-p)}{p}} \left(-f dt^2 + \sum_{i=1}^p dx_i^2 + \frac{\tilde{r}_0^{7-p}}{\tilde{r}^{7-p}} \frac{d\tilde{r}^2}{f} \right). \quad (\text{A.9})$$

Finally, by changing a variable $\tilde{r} = \left(\frac{(p-5)^2 \tilde{r}_0^{p-7}}{4} \right)^{1/(p-5)} r^{\frac{2}{p-5}}$, we arrive at

$$ds_{p,E}^2 = a r^{\frac{2(9-p)}{p(p-5)}} \left(-f dt^2 + \sum_{i=1}^p dx_i^2 + \frac{dr^2}{f} \right), \quad f = 1 - \left(\frac{r}{r_H} \right)^{-\frac{2(7-p)}{p-5}}, \quad (\text{A.10})$$

where $a = \left(\frac{p-5}{2}\right)^{\frac{2}{p-5}} R^{-\frac{2(8-p)}{p}} (\tilde{r}_0)^{\frac{5(p-7)}{p(p-5)}}$ and the r dependent factor in emblackening factor can be identified as $-2(7-p)/(p-5) = d+z-\theta$. Compared to the metric (2.1), we conclude

$$d = p, \quad \theta = \frac{(p-3)^2}{p-5}, \quad z = 1. \quad (\text{A.11})$$

This case has a positive dynamical exponent $z = 1$ as we expected. The corresponding temperature and entropy of the reduced effective geometry are

$$\begin{aligned} T &= \frac{f'(r_H)}{4\pi} = \frac{|d+z-\theta|}{4\pi r_H} = \frac{1}{2\pi r_H} \left| \frac{7-p}{5-p} \right|, \\ S &= \frac{1}{4G_p} a^{p/2} V_p r_H^{-\frac{9-p}{5-p}} \sim T^{\frac{9-p}{5-p}} = T^{\frac{d-\theta}{z}}. \end{aligned} \quad (\text{A.12})$$

The temperature and entropy (A.12) are the same as those evaluated in (A.4) if one correctly identifies the parameters before and after the dimensional reduction.

A.2 Black M2 brane

Similarly we consider the dimensional reduction of the black M2 brane solution and its dimensional reduction to 4 dimensions. The 11 dimensional M2 brane metric is

$$\begin{aligned} S &= \frac{1}{2\kappa_{11}^2} \int d^{11}x \sqrt{-g} \mathcal{R} - \frac{1}{4\kappa_{11}^2} \int \left(F_4 \wedge *F_4 + \frac{1}{3} A_3 \wedge F_4 \wedge F_4 \right), \\ ds_{M2}^2 &= H^{-2/3} \left(-f dt^2 + \sum_{i=1}^2 dx_i^2 \right) + H^{1/3} \left(\frac{d\tilde{r}^2}{f} + \tilde{r}^2 d\Omega_7^2 \right), \\ H &= 1 + \frac{R^6}{\tilde{r}^6}, \quad f = 1 - \frac{\tilde{r}_H^6}{\tilde{r}^6}, \quad *F_4 = F_7 = 6R^6 V(S^7). \end{aligned} \quad (\text{A.13})$$

This metric is explicitly given in [37]. The quantization condition is $R^9 \pi^5 = \sqrt{2} N^{3/2} \kappa_{11}^2$. The temperature and entropy of the geometry are

$$T = \frac{3}{2\pi} \frac{\tilde{r}_H^2}{R^3}, \quad S = \frac{8\sqrt{2}\pi^2}{27} V_2 N^{3/2} T^2, \quad (\text{A.14})$$

where we use the explicit expression $V(S^7) = \frac{\pi^4}{3}$.

We compactify the solution on S^7 . Typically for the conformal cases, the dimensional reduction does not introduce any extra radial dependence on the field theory coordinates. Thus the resulting action becomes $S = \frac{1}{2\kappa_4^2} \int d^4x \sqrt{-g_4} \mathcal{R}_4 + \dots$ with $\frac{1}{2\kappa_4^2} = \frac{R^7 V(S^7)}{2\kappa_{11}^2}$. And the corresponding Einstein frame metric is nothing but the original metric (A.13) without the last term $d\Omega_7^2$. By changing a variable $\tilde{r} = \frac{1}{\sqrt{2}} R^{3/2} r^{-1/2}$, we get

$$ds_E^2 = \frac{R^2}{4r^2} \left(-f dt^2 + \sum_{i=1}^2 dx_i^2 + \frac{dr^2}{f} \right), \quad f = 1 - \frac{r^3}{r_H^3}. \quad (\text{A.15})$$

Compared to the metric (2.1), we conclude

$$d = 2, \quad \theta = 0, \quad z = 1, \quad (\text{A.16})$$

which show $z = 1$ and $\theta = 0$ as we expected. The corresponding temperature and entropy of the reduced effective geometry are

$$T = \frac{3}{4\pi r_H}, \quad S = \frac{\pi^2 R^2}{9G_4} V_2 T^2, \quad (\text{A.17})$$

where the temperature and the entropy are the same as those of the original M2 brane if we consider the relation $\tilde{r}_H = \frac{1}{\sqrt{2}} R^{3/2} r_H^{-1/2}$ and use the reduction $\frac{1}{2\kappa_4^2} = \frac{1}{16\pi G_4} = \frac{R^7 V_7}{2\kappa_{11}^2}$.

A.3 Black M5 brane

The 11 dimensional M5 brane action and metric are

$$S = \frac{1}{2\kappa_{11}} \int d^{11}x \sqrt{-g} \mathcal{R} - \frac{1}{4\kappa_{11}} \int \left(F_4 \wedge *F_4 + \frac{1}{3} A_3 \wedge F_4 \wedge F_4 \right), \quad (\text{A.18})$$

$$ds_{M5}^2 = H^{-1/3} \left(-f dt^2 + \sum_{i=1}^5 dx_i^2 \right) + H^{2/3} \left(\frac{d\tilde{r}^2}{f} + \tilde{r}^2 d\Omega_4^2 \right), \quad (\text{A.19})$$

$$H = 1 + \frac{R^3}{\tilde{r}^3} \rightarrow \frac{R^3}{\tilde{r}^3}, \quad f = 1 - \frac{\tilde{r}_H^3}{\tilde{r}^3}, \quad F_4 = dA_3 = 3R^3 V(S^4).$$

The temperature and entropy of the geometry are

$$T = \frac{3}{4\pi} \frac{\tilde{r}_H^{1/2}}{R^{3/2}}, \quad S = \frac{2^7 \pi^3}{3^6} V_5 N^3 T^5, \quad (\text{A.20})$$

where we use $V(S^4) = \frac{8\pi^2}{3}$ and the quantization condition $R^9 \pi^5 2^7 = N^3 \kappa_{11}^2$.

Upon compactifying down to 7 dimensions, the action becomes $S = \frac{1}{2\kappa_7^2} \int d^7x \sqrt{-g_7} \mathcal{R}_7 + \dots$ with $\frac{1}{2\kappa_7^2} = \frac{R^4 V(S^4)}{2\kappa_{11}^2}$. Similar to the M2 brane, the resulting metric becomes

$$ds_E^2 = \frac{4R^2}{r^2} \left(-f dt^2 + \sum_{i=1}^5 dx_i^2 + \frac{dr^2}{f} \right), \quad f = 1 - \frac{r^6}{r_H^6}, \quad (\text{A.21})$$

after changing a variable $\tilde{r} = 4R^3 r^{-2}$. Compared to the standard form of the metric (2.1), we conclude

$$d = 5, \quad \theta = 0, \quad z = 1. \quad (\text{A.22})$$

This case has a positive dynamical exponent $z = 1$ and $\theta = 0$ as we expected. The corresponding temperature and entropy of the reduced effective geometry are

$$T = \frac{6}{4\pi r_H}, \quad S = \frac{2^8 \pi^5 R^5}{3^5 G_7} V_5 T^5, \quad (\text{A.23})$$

where the temperature and the entropy are the same as those of the original M5 brane if we consider the relation $\tilde{r}_H = 4R^3 r_H^{-2}$ and use the reduction $\frac{1}{2\kappa_7^2} = \frac{R^5 V(S^5)}{16\pi G_{11}}$.

A.4 Dp-D(p+4) branes

In this section we would like to consider the intersecting Dp-Dq, $q = p+4$, $p = 0, 1, 2$ solutions [120][121][122], studied recently in the context of the hyperscaling violation solution [16].

$$ds_{pq}^2 = \frac{1}{\sqrt{H_p H_q}} [-dt^2 + \sum_{i=1}^p dx_i^2] + \sqrt{\frac{H_p}{H_q}} \sum_{j=p+1}^{p+4} dx_j^2 + \sqrt{H_p H_q} [d\rho^2 + \rho^2 d\Omega_{4-p}^2] , \quad (\text{A.24})$$

$$e^\Phi = H_p^{\frac{3-p}{4}} H_q^{-\frac{p+1}{4}} , \quad H_{p,q} = 1 - \frac{Q_{p,q}}{\rho^{3-p}} , \quad (\text{A.25})$$

$$A_{p+1} = (1 - H_p^{-1}) dt \wedge dx^1 \wedge \cdots \wedge dx^p , \quad (\text{A.26})$$

$$A_{p+5} = (1 - H_q^{-1}) dt \wedge dx^1 \wedge \cdots \wedge dx^{p+4} , \quad (\text{A.27})$$

We would like to take the near horizon limit first, $H_p H_q = H^2 = \frac{Q^2}{\rho^{2(3-p)}}$, $Q^2 = Q_p Q_q$, and dimensionally reduce to the Einstein metric to $p+6$ dimensions, using $ds_E^2 = H^{\frac{p+2}{p+4}} \rho^{\frac{2(4-p)}{p+4}} ds_{str}^2$.

$$ds_{pq,E}^2 = Q_p^{\frac{-3}{p+4}} Q_q^{\frac{2}{p+4}} \rho^{\frac{14-4p}{p+4}} \left(-dt^2 + \sum_{i=1}^p dx_i^2 + \frac{Q_p}{\rho^{3-p}} \sum_{j=p+1}^{p+4} dx_j^2 + \frac{Q_p Q_q}{\rho^{2(3-p)}} d\rho^2 \right) . \quad (\text{A.28})$$

Using $\rho = \left(\frac{Q}{2-p}\right)^{\frac{1}{2-p}} u^{\frac{1}{2-p}}$ for $p < 2$, we obtain

$$ds_{pq,E}^2 = u^{\frac{14-4p}{(p+4)(2-p)}} \left(-dt^2 + \sum_{i=1}^p dx_i^2 + u^{\frac{p-3}{2-p}} \sum_{j=1}^4 dx_j^2 + \frac{du^2}{u^4} \right) , \quad (\text{A.29})$$

where we omit the overall factor $Q_p^{\frac{-3}{p+4}} Q_q^{\frac{2}{p+4}} \left(\frac{Q}{2-p}\right)^{\frac{14-4p}{(2-p)(p+4)}}$ and absorb $Q_p \left(\frac{Q}{2-p}\right)^{\frac{p-3}{2-p}}$ factors to x_j . This metric reveals that spatial anisotropic exponent is necessary to describe the string theory solutions with two dimensionful parameters. Compared to the standard metric (1.2), we conclude

$$d = p + 4 , \quad \theta = \frac{1-p^2}{2-p} , \quad z = 1 , \quad \sharp = \frac{1-p}{2(2-p)} . \quad (\text{A.30})$$

This is one of the main example to reveal the spatial anisotropic exponent advertised in the introduction. Surely this example has two independent dimensionful parameters. Effectively, one can be absorbed in the front factor to the hyperscaling violation exponent, while the other one is pushed into some part of the spatial coordinates with spatial anisotropic exponent. Until now we consider the dimensional reduction to $p+6$ dimensions to show the manifestation of the advertised spatial anisotropic exponent.

Now for the coordinates $(p+1) - (p+4)$ are compact, this metric can be further dimensionally reduced down to $p+2$ dimensions. Similarly, we obtain

$$ds_{p,E}^2 = (Q_p Q_q)^{\frac{2}{p(2-p)}} \left(\frac{1}{2-p}\right)^{\frac{2}{p(2-p)}} u^{\frac{2}{p(2-p)}} \left(-dt^2 + \sum_{i=1}^p dx_i^2 + \frac{du^2}{u^4} \right) . \quad (\text{A.31})$$

Comparing to the standard metric (1.2), we conclude

$$d = p, \quad \theta = -\frac{(1-p)^2}{2-p}, \quad z = 1. \quad (\text{A.32})$$

Considering the finite temperature generalization with the emblackening factor

$$f = 1 - \frac{\rho_H^{3-p}}{\rho^{3-p}} = 1 - \left(\frac{u_H}{u}\right)^{\frac{3-p}{2-p}}, \quad (\text{A.33})$$

we again check that $d + z - \theta = \frac{3-p}{2-p}$.

D1D5 system

Let us concentrate on the conformal case with $p = 1$. This geometry shows an interesting property, which can be clearly seen in the following form

$$ds_{D1D5}^2 = \frac{\rho^2}{Q}[-f dt^2 + dx_1^2] + \frac{Q}{\rho^2} \frac{d\rho^2}{f} + Q d\Omega_3^2 + \sqrt{\frac{Q_1}{Q_5}} ds_{M_4}^2, \quad (\text{A.34})$$

which is $AdS_3 \times S^3 \times M_4$. We check that there is no hyperscaling violation when we take dimensional reductions along the directions S^3 .

$$ds_{D1D5}^2 = Q\rho^2[-f dt^2 + dx_1^2 + \frac{1}{\rho^4} \frac{d\rho^2}{f} + \frac{Q_1}{\rho^2} ds_{M_4}^2], \quad (\text{A.35})$$

which is already in a standard form because the boundary sits at $u \rightarrow \infty$. Thus we get

$$d = 5, \quad \theta = 0, \quad z = 1, \quad \sharp_{M_4|1} = 0. \quad (\text{A.36})$$

Note that normally we expect to get $\sharp = 1$ to have rotationally invariant metric. Thus $\sharp_{M_4|1} = 0$ reveals the spatial anisotropy. For the effective metric $AdS_3 \times M_4$, we observe a different scale between the two spaces AdS_3 and M_4 . This is manifested in the prefactors 1 and $\frac{Q_1}{\rho^2}$ in (A.35). This picture would be applicable for non-compact M_4 as well as compact M_4 for the physical cases requiring compact coordinates.

Now let us take the dimensional reductions further along the directions M_4 for the compact $M_4 = T^4$. Then we arrive ($u = \rho$)

$$ds_E^2 \propto \rho_1 \rho_5 u^2 \left(-f dt^2 + dx_1^2 + \frac{1}{u^4} \frac{du^2}{f} \right), \quad (\text{A.37})$$

where a single scale $\rho_1 \rho_5$ is absorbed into the coordinates t, x_1 . It is clear that the boundary is at $\rho \rightarrow \infty$ from the coordinate x_1 , and thus the corresponding exponents are $\theta = 0, z = 1$ for $d = 1$. It is worthwhile to mention that this case falls into an interesting case $\theta = d - 1$ for the Lifshitz type theories trivially. As already mentioned, this case falls into the conformal case and we don't expect to have any physically relevant scale.

This system still satisfy the relation $d + z - \theta = 2$, which is the power behavior of the emblackening factor. Note that this system is related to a conformal case, which is signified by $\theta = 0$, in contrast with the case of D1 brane $\theta = -1, z = 1$ for $d = 1$ given in (A.11).

A.5 Intersecting and interpolating M-branes

In this section we would like to consider an intersecting M2-M5 solution [123] and an interpolating background between $2\perp 2$ and $2\perp 5$ [121]. Some of them are considered recently in [14]. Here we observe that these intersecting and interpolating solutions reveal the necessity of the spatial anisotropic exponent(s) \sharp .

Intersecting solution

Let us first start with the intersecting M2-M5 solution [123].

$$ds_{M2M5}^2 = H_2^{-2/3} H_5^{-1/3} (-dt^2 + dx_1^2) + H_2^{-2/3} H_5^{2/3} (dx_2^2) + H_2^{1/3} H_5^{-1/3} (dx_3^2 + \dots + dx_6^2) + H_2^{1/3} H_5^{2/3} [d\rho^2 + \rho^2 d\Omega_3^2] , \quad (\text{A.38})$$

$$H_{p,q} = 1 + \frac{Q_{p,q}}{\rho^2} , \quad F_{r012} = \pm \partial_\rho H_2^{-1} , \quad F_{r\alpha\beta\gamma} = \pm \epsilon_{\alpha\beta\gamma} \partial_\rho H_5 . \quad (\text{A.39})$$

After taking the near horizon limit, we get

$$ds_{M2M5}^2 = Q_2^{-2/3} Q_5^{-1/3} \rho^2 (-dt^2 + dx_1^2) + Q_2^{-2/3} Q_5^{2/3} (dx_2^2) + Q_2^{1/3} Q_5^{-1/3} (dx_3^2 + \dots + dx_6^2) + Q_2^{1/3} Q_5^{2/3} \rho^{-2} [d\rho^2 + \rho^2 d\Omega_3^2] . \quad (\text{A.40})$$

Here the geometry is factorized into the product of an AdS_3 spacetime, a three-sphere S^3 , and a flat Euclidean five-dimensional space E^5 [123].

We dimensionally reduce the compact coordinates to the Einstein metric in 8 dimensions. Using $ds_E^2 = (Q_2^{1/2} Q_5)^{1/3} ds_{str}^2$, we get

$$ds_{25,E}^2 = Q_2^{1/2} Q_5 \rho^2 \left(-dt^2 + dx_1^2 + \frac{1}{\rho^2} (dx_2^2 + dx_3^2 + \dots + dx_6^2) + \frac{d\rho^2}{\rho^4} \right) , \quad (\text{A.41})$$

where we absorb Q factors in the spatial coordinates x_2, \dots, x_6 and redefine $\rho \rightarrow \sqrt{Q_2 Q_5} \rho$. This is already in a standard form and we can read off the exponents as

$$d = 7 , \quad \theta = 0 , \quad z = 1 , \quad \sharp = 0 . \quad (\text{A.42})$$

The fact $\theta = 0$ is consistent with the observation that the near horizon geometry is $\text{AdS}_3 \times E^5 \times S^3$. Note that $\sharp = 0$ is non-trivial, and provide an example to generate the spatial anisotropic exponent. There are other examples listed in [123]. We expect to get the similar results.

Interpolating background

Now, let us turn to the interpolating background between $2\perp 2$ and $2\perp 5$ [121].

$$ds^2 = \tilde{H}_3^{1/3} H_3^{1/3} H_1^{1/3} [-H_1^{-1} H_3^{-1} dt^2 + H_1^{-1} dx_1^2 + H_3^{-1} (dx_2^2 + dx_3^2) + \tilde{H}_3^{-1} H_3^{-1} dx_5^2 + \tilde{H}_3^{-1} (dx_4^2 + dx_{11}^2) + d\rho^2 + \rho^2 d\Omega_3^2] , \quad (\text{A.43})$$

where $H_i = 1 + \frac{Q_i}{\rho^2}$ and $\tilde{H}_3 = 1 + \frac{\tilde{Q}_3}{\rho^2}$. After taking the near horizon limit, we get

$$ds^2 = \frac{\tilde{Q}_3^{1/3} Q_3^{1/3} Q_1^{1/3}}{\rho^2} \left[-\frac{\rho^4}{Q_1 Q_3} dt^2 + \frac{\rho^2}{Q_1} dx_1^2 + \frac{\rho^2}{Q_3} (dx_2^2 + dx_3^2) \right. \\ \left. + \frac{\rho^4}{\tilde{Q}_3 Q_3} dx_5^2 + \frac{\rho^2}{\tilde{Q}_3} (dx_4^2 + dx_{11}^2) + d\rho^2 + \rho^2 d\Omega_3^2 \right], \quad (\text{A.44})$$

We dimensionally reduce the compact coordinates to the Einstein metric in 8 dimensions. Using $ds_E^2 = (Q_1 Q_3 \tilde{Q}_3)^{1/6} ds_{str}^2$, we get

$$ds_{25,E}^2 = (Q_1 Q_3 \tilde{Q}_3)^{1/2} \rho^2 \left[-dt^2 + dx_5^2 + \frac{1}{\rho^2} (dx_2^2 + dx_3^2 + dx_4^2 + dx_{11}^2) + \frac{d\rho^2}{\rho^4} \right], \quad (\text{A.45})$$

where we absorb Q factors in the coordinates $t, x_1, \dots, x_5, x_{11}$. Thus we check this metric is the same as (A.41) and thus

$$d = 7, \quad \theta = 0, \quad z = 1, \quad \sharp_{i|1} = 0, \quad (\text{A.46})$$

where $i = 2, \dots, 6$. Again, note that $\sharp = 0$ is non-trivial, and provide an example to generate the spatial anisotropic exponent.

B Dimensional reduction of solutions with Schrödinger scaling

Let us consider the dimensional reduction of the theories with Schrödinger scaling. These are mostly at zero temperature. They are constructed by null Melvin twist [88][89], which serves as an effective way to generate non-relativistic solutions with Schrödinger isometry, starting from the known relativistic solutions. Most of the solutions we consider are listed in [90].¹⁵ Non-relativistic Dp branes are analyzed in detail in the main body, including their finite temperature generalizations §3.

There exists an interesting solution, type IIA NS5 brane in §B.2, among the solutions we consider, which satisfies the following condition

$$\frac{\theta}{D} = \frac{d+1-z}{d+1}, \quad D = d+1 = 5, \quad \theta = 3. \quad (\text{B.1})$$

This solution is expected to possess Fermi surfaces in the dual field theory in the context of Schrödinger type theories [11], similar to the Lifshitz type theories [6][7][8]. This is the first explicit example belong to this class from the top down string theory solutions with Schrödinger isometry.

¹⁵We are grateful to Yaron Oz for his numerous advices and valuable comments especially on this section.

B.1 ‘Conformal’ cases

We consider the null Melvin twist of the conformal branes including M2, M5, D3, D1D5, F1NS5 systems [90]. All the non-relativistic conformal branes share the property that the part of the metric along the internal directions are independent of the radial coordinates, and the associated dilaton is either not present or constant. Thus we can write a general form of the metric at zero temperature as

$$ds^2 = \left(\frac{\rho_p}{r}\right)^2 \left(-\frac{\tilde{\Delta}^2}{r^{2z-2}} dt^2 - 2dt d\xi + \sum_{i=1}^{p-1} \eta_i dx_i^2 + dr^2 \right) + \rho_p^2 d\Omega^2, \quad (\text{B.2})$$

where $d = p - 1$. For example, $\rho_p = \rho_2$, $\tilde{\Delta} = 2\beta\rho_2$, $p = 2$, $\eta_i = 1$ and $d\Omega^2 = d\Omega_7^2$ for non-relativistic M2 brane, while $\rho_p^2 = \rho_1\rho_5$, $\tilde{\Delta} = \beta\rho_1\rho_5$, $p = 5$, $\eta_i = r^2/\rho_5^2$ and $d\Omega^2 = d\Omega_3^2$ for D1D5 system. We observe a clear distinction between these two cases: D1D5 has explicit radial dependence in η_i , which can not be removed by redefining the radial coordinate.

The dimensional reduction along the coordinates $d\Omega^2$ does not produce any radial dependence. Thus the resulting metric is the same as before, which is (B.2) without the last term. We list various exponents of these cases by comparing to the standard form (1.1) with $a = 1$, $b = 1$ and $D = d + 1$ (after absorbing the dimensionful parameter $\tilde{\Delta}$ into dt).

$$\text{D3 :} \quad d = 2, \quad \theta = 0, \quad z = 2, \quad (\text{B.3})$$

$$\text{M2 :} \quad d = 1, \quad \theta = 0, \quad z = 3/2, \quad (\text{B.4})$$

$$\text{M5 :} \quad d = 4, \quad \theta = 0, \quad z = 3, \quad (\text{B.5})$$

$$\text{D1D5 :} \quad d = 0 + 4, \quad \theta = 0, \quad z = 2, \quad (\text{B.6})$$

$$\text{F1NS5 :} \quad d = 0 + 4, \quad \theta = 0, \quad z = 2. \quad (\text{B.7})$$

All the cases reveal $\theta = 0$. M2 and M5 cases reveal interesting variations in dynamical exponents and do not have special non-relativistic conformal symmetry, which is clear from the non-trivial dynamical exponent. It will be interesting to investigate these cases further from this point of view.

The last two cases, (B.6) and (B.7), are different because the spatial dimensions have explicit radial dependence. After dimensional reduction, the metric is

$$ds_{D1D5}^2 = \left(\frac{\rho_p}{r}\right)^2 \left(-\frac{\tilde{\Delta}^2}{r^2} dt^2 - 2dt d\xi + dr^2 \right) + ds_{M_4}^2. \quad (\text{B.8})$$

To make this metric in the form (1.1) with $\eta_i = 1$, it is required to change coordinate with non-polynomial type, $r \sim e^y$. Thus dynamical exponent is not determined. Thus this metric has neither the Galilean boost, nor the special conformal transformations. To have nontrivial \sharp , we need more general intersecting D-branes.

The finite temperature generalizations for D1D5 and F1NS5 systems can be considered similarly. These metrics generate the ‘ K ’ factor similar to (3.7), which might spoil some of the properties of the zero temperature. It turns out that the K -factors become constant in the near horizon limit [90], which is special for this case.

B.2 NS5A brane

In this section, we consider the non-relativistic version of the type IIA NS5 brane solution at zero temperature in some detail. This case turns out to be a very interesting case, being expected to possess Fermi surface according to recent conjecture [6][7].

The metric and dilaton are given in [90]

$$ds^2 = -\frac{2\Delta^2}{\tilde{r}^2}dt^2 - 2dtd\xi + \sum_{i=1}^4 dx_i^2 + \frac{\rho_5}{\tilde{r}}(d\tilde{r}^2 + \tilde{r}^2 d\Omega_3^2), \quad e^\Phi = \left(\frac{\tilde{r}}{\rho_5}\right)^{3/2}, \quad (\text{B.9})$$

where we omit the other fields. We compactify this solution on S^3 and get the Einstein metric in 7 dimensions

$$ds_E^2 = 4^{3/5}\rho_5^{12/5}r^{-6/5}\left(-\frac{\tilde{\Delta}^2}{r^4}dt^2 - 2dtd\xi + \sum_{i=1}^4 dx_i^2 + dr^2\right), \quad (\text{B.10})$$

where we use $ds_E^2 = \rho_5^{9/5}\tilde{r}^{-3/5}ds^2$, $\tilde{r} = \frac{r^2}{4\rho_5}$ and $\tilde{\Delta} = 32\rho_5^2\Delta^2$. Compared to the standard metric (1.1), we get

$$d = 4, \quad \theta = 2, \quad z = 3, \quad (\text{B.11})$$

which belongs to the category of logarithmic violation case with the condition

$$\frac{\theta}{D} = \frac{d+1-z}{d+1}, \quad (\text{B.12})$$

where $D = d + 1$. What is so special about this metric? It turns out that the holographic stress energy tensor has some distinctive signature along with the entanglement entropy. We further analyze this case in some detail here.

Entanglement entropy

Entanglement entropy has become a new useful tool to classify and understand different phases of field theory. For example, it differentiates the fermionic models from the bosonic ones [45]. This is extensively investigated in the context of holography [46].

The entanglement entropy can be computed using the minimal surface prescription of the ‘codimension 2 holography’ utilizing the stationary ADM form, developed in [11]

$$ds_E^2 = 4^{3/5}\rho_5^{12/5}r^{-6/5}\left(-\frac{\tilde{\Delta}^2}{r^4}\left(dt + \frac{r^4}{\tilde{\Delta}^2}d\xi\right)^2 + \frac{r^4}{\tilde{\Delta}^2}d\xi^2 + \sum_{i=1}^4 dx_i^2 + dr^2\right), \quad (\text{B.13})$$

with the condition $dt + \frac{r^4}{\tilde{\Delta}^2} d\xi = 0$. The entanglement entropy is given by (see the details in §4 of [11])

$$\mathcal{S} = \frac{M_{Pl}^5}{4} \frac{8\rho_5^6}{\tilde{\Delta}} \left(\frac{L^3}{M_\xi} \right) \log \left(\frac{2l}{\epsilon} \right). \quad (\text{B.14})$$

This result shows the logarithmic violation of entanglement entropy. This important property is associated with the conjecture [6][7] that “the entanglement entropies of the system with Fermi surface show the logarithmic violation of the area law.”

Holographic stress energy tensor

Holographic stress energy tensor in the context of Schrödinger holography is computed using Brown-York method in §2.3 of [11]. We summarize the result here (using the same notations of [11]).

$$\langle \hat{\tau}_{tt} \rangle = -\frac{1}{r_c^{1+z}} h_{00}, \quad \langle \hat{\tau}_{t\xi} \rangle = \langle \hat{\tau}_{\xi t} \rangle = -\frac{z}{r_c^{1+z}} h_{t\xi}, \quad \langle \hat{\tau}_{ij} \rangle = -\frac{z}{r_c^{1+z}} h_{ij}. \quad (\text{B.15})$$

In particular, the coefficient of $\langle \hat{\tau}_{tt} \rangle$ becomes unity and is independent of parameters, z, θ, d and D . Let us compare this to the extensive violation case $\theta = d + 2 - z$ for $D = d + 1$. Then

$$\langle \hat{\tau}_{tt} \rangle = 0, \quad \langle \hat{\tau}_{t\xi} \rangle = \langle \hat{\tau}_{\xi t} \rangle = -\frac{z-1}{r_c^z} h_{t\xi}, \quad \langle \hat{\tau}_{ij} \rangle = -\frac{z-1}{r_c^z} h_{ij}. \quad (\text{B.16})$$

We also observe the coefficient of $\langle \hat{\tau}_{tt} \rangle$ is independent of the parameters.

These coefficients of the holographic stress energy tensor are independent of the the normalization and thus universal. Thus we expect that these provide some important properties in further investigating the physical significances of the theories for the range $d + 1 - z \leq \theta \leq d + 2 - z$ for $D = d + 1$.

Scalar correlation functions

The equation of motion for a scalar field with mass m in the background (B.10) is given (in the momentum space) as

$$\left(\partial_r^2 - \frac{3}{r} \partial_r - \vec{k}^2 + 2M\omega - \beta \frac{M^2}{r^4} - \frac{m^2}{r^{6/5}} \right) \phi = 0, \quad (\text{B.17})$$

where \vec{k} and ω are Fourier transform of \vec{x} and t , respectively. We treat the ξ direction special and replace $\partial_\xi = iM$ for the scalar field following [11].

It is clear that the asymptotic expansion is not well posed with the polynomial form due to the term proportional to M^2 . Many of the interesting cases have similar difficulties for computing the correlation functions. This can be interpreted as a signal that the geometry

is not valid all the way to the boundary, thus the asymptotic expansion can not be trusted. Thus we would like to evaluate the semiclassical propagator.

Semiclassical propagators

Semiclassical propagators of the Schrödinger type backgrounds are studied in detail in §2.2 of [11]. For the Schrödinger type metric, there are three different types of propagator. All the results are valid in the limit where the second exponential factors are suppressed.

One can evaluate the static semiclassical propagator as

$$G(\Delta x_i) \sim \exp \left[2m \frac{D}{\theta} \epsilon^{\theta/D} \right] \exp \left[-m \frac{D}{\theta} c_{\theta/D} |\Delta x_i|^{\theta/D} \right], \quad (\text{B.18})$$

where $c_{\theta/D}$ only depends on the combination θ/D and given in equation (2.22) of [11]. The static case only depends on the combination $\theta/D = 2/5$, independent of other parameters. Note the non-trivial dependence of the propagator on the hyperscaling violation exponent θ .

Due to the cross term present in the metric (B.10), there is also a stationary propagator. In general, this case is rather complicated. This simplifies when we constrain the travel distance along the ξ coordinate to be the total length L_ξ , which is the defining length associated with the dual particle number M_ξ . Then

$$G(L_\xi) \sim \exp \left[2m \frac{D}{\theta} \epsilon^{\theta/D} \right] \exp \left[-2m \frac{D}{\theta} \hat{c}_{L_\xi} L_\xi^{\frac{\theta}{(z-2)D}} \right], \quad (\text{B.19})$$

where \hat{c}_{L_ξ} is given in equation (2.33) of [11]. The correlation function can not decay faster than this because there exist the maximum distance L_ξ in ξ direction. This is a unique property of the Schrödinger type theories.

The timelike propagator is also complicated in general, which can be found in §2.2 of [11]. Thus we consider the special case, where the constant of motion along ξ coordinate is small. The result of the timelike propagator is

$$G(\Delta t) \sim \exp \left[2m \frac{D}{\theta} \epsilon^{\theta/D} \right] \exp \left[-2m \frac{D}{\theta} c_\xi |\Delta t|^{\frac{\theta}{2D-\theta}} \right], \quad (\text{B.20})$$

where c_ξ is given in equation (2.43) of [11].

Typically the semiclassical propagators are exponentially suppressed in the valid regime, accordingly for $-2m|\Delta x_i|^{\theta/D} \gg 1$, $-2mL_\xi^{\frac{\theta}{(z-2)D}} \gg 1$ and $-2m|\Delta t|^{\frac{\theta}{2D-\theta}} \gg 1$. Still it is possible to get the standard form $G \sim \exp \left[-m \left(\frac{|\Delta x_i|^2}{2|\Delta t|} \right)^{\frac{\theta}{(z-2)D}} \right]$ for the general case [11].

Further investigations of this case would be very interesting to figure out whether these systems possess some physically distinctive properties.

B.3 NS5B brane

Let us consider type IIB NS5 brane solution in 10 dimensions [90]. The metric and dilaton are

$$ds_{NS5A}^2 = -\frac{2\Delta^2}{\tilde{r}^2} dt^2 - 2dt d\xi + \sum_{i=1}^4 dx_i^2 + \frac{\rho_5}{\tilde{r}^2} (d\tilde{r}^2 + \tilde{r}^2 d\Omega_3^2) , \quad e^\Phi = \frac{\tilde{r}}{\rho_5} , \quad (\text{B.21})$$

where we omit other irrelevant fields again. We compactify this solution on S^3 down to 7 dimensions. The resulting metric in Einstein frame is given by

$$ds_E^2 \sim \tilde{r}^{-4/5} \left(-\frac{2\Delta^2}{\tilde{r}^2} dt^2 - 2dt d\xi + \sum_{i=1}^4 dx_i^2 + \frac{\rho_5}{\tilde{r}^2} d\tilde{r}^2 \right) , \quad (\text{B.22})$$

where we use $ds_E^2 \sim \tilde{r}^{-4/5} ds^2$. Apparently, we can not put this metric in the standard form (1.1) with the reference coordinate, because it is necessary to make a coordinate transformation with exponential form $\tilde{r} \sim e^{ar}$. Thus the power law scaling properties do not hold anymore. This case is briefly outlined in footnote 5 in general context.

Let us consider this case more closely. One can pull ρ_5 out of the parenthesis and absorb it into other field theory coordinates appropriately, without modifying the radial dependence of the metric. There seems no preferred scaling for the radial coordinate, yet we would take it as a reference scale $r \rightarrow \lambda r$. With these discussion, we can put the metric in, yet, another standard form as

$$ds^2 = r^{2\theta/D} \left(-r^{-2z} dt^2 - 2dt d\xi + \frac{dr^2}{r^2} + \sum_{i=1}^d dx_i^2 \right) , \quad (\text{B.23})$$

where the scaling symmetry of this metric is given by

$$t \rightarrow \lambda^z t , \quad \xi \rightarrow \lambda^{-z} \xi , \quad r \rightarrow \lambda r , \quad x_i \rightarrow x_i . \quad (\text{B.24})$$

From this metric, it is not clear whether there is precise meaning of dynamical exponent because the spatial directions do not scale. Thus this types of metric does not possess scaling symmetries of the kind we consider here.

B.4 F1 brane

F1 brane solution in 10 dimensions is described by the metric and dilation [90]

$$ds^2 = \left(\frac{\rho_0}{\tilde{r}} \right)^6 \left[-\frac{2\Delta^2}{\tilde{r}^2} dt^2 - 2dt d\xi \right] + \left(\frac{\rho_0}{\tilde{r}} \right)^4 (d\tilde{r}^2 + \tilde{r}^2 d\Omega_7^2) , \quad e^\Phi = \left(\frac{\rho_0}{\tilde{r}} \right)^3 , \quad (\text{B.25})$$

where we omit other irrelevant field contents. We compactify this solution on S^7 down to 3 dimensional Einstein metric

$$ds_E^2 \sim r^{-4} \left(-\frac{\tilde{\Delta}^2}{r} dt^2 - 2dt d\xi + dr^2 \right), \quad (\text{B.26})$$

where we use $\tilde{r} = \sqrt{r}$. Note that the naive identification of the dynamical exponent shows $z = \frac{1}{2}$, which actually violate the null energy condition. A moment of thought tells that the meaning of the dynamical exponent is not well posed because there is no spatial directions left after the dimensional reduction. Furthermore, there can not be symmetries for the Galilean boost and special conformal transformation.

B.5 KK monopole

Let us consider the metric of the KK monopole in 11 dimensional Einstein frame [90]

$$ds_{KK}^2 = -\frac{2\Delta^4}{\tilde{r}^4} dt^2 - 2dt d\xi + \sum_{i=1}^5 dx_i^2 + \left(\frac{\rho_0}{\tilde{r}}\right)^4 (d\tilde{r}^2 + \tilde{r}^2 d\Omega_3^2). \quad (\text{B.27})$$

One might prefer to view that the metric approaches to the boundary for $\tilde{r} \rightarrow 0$. Yet the situation is not clear once we perform the dimensional reduction.

We compactify this on S^3 . The resulting 8 dimensional Einstein metric is

$$ds_E^2 \sim \tilde{r}^{-1} \left(-\frac{2\Delta^4}{\tilde{r}^4} dt^2 - 2dt d\xi + \sum_{i=1}^5 dx_i^2 + \left(\frac{\rho_0}{\tilde{r}}\right)^4 d\tilde{r}^2 \right), \quad (\text{B.28})$$

where we use $ds_E^2 = \tilde{r}^{-1} ds^2$. To get the standard form (1.1), we change a variable $\tilde{r} = \frac{1}{r}$. Then we get

$$ds_E^2 \sim r \left(-r^4 dt^2 - 2dt d\xi + \sum_{i=1}^5 dx_i^2 + dr^2 \right). \quad (\text{B.29})$$

Compared to the standard metric (1.1), we obtain

$$d = 5, \quad \theta = 9, \quad z = -1, \quad (\text{B.30})$$

where we use $D = 6$. Note that the dynamical exponent is negative and the hyperscaling exponent is a relative large positive number.

To be more careful, we also try to put the metric in another form using the u coordinate as in footnote 4. It turns out that the metric (B.28) is already in a standard form given in footnote 4. Thus we put $u = \tilde{r}$, then we get

$$ds_E^2 \sim u^{-1} \left(-\frac{1}{u^4} dt^2 - 2dt d\xi + \sum_{i=1}^5 dx_i^2 + \frac{1}{u^4} du^2 \right), \quad (\text{B.31})$$

where we absorb various constants into the appropriate coordinates. According to the standard form there, we obtain the same exponents as (B.30).

Thus we conclude that the KK monopole solution has a negative dynamical exponent. Can we understand the negative dynamical exponent, which means that space and time scale in an opposite way? Some thoughts give an observation that the standard forms given in (B.29) and (B.31) may not appropriately reflect the location of the boundary, meaning that the r coordinate in (B.29) describe the boundary at $r \rightarrow \infty$ and thus can be described more appropriately by u coordinate, and vice versa. But there is no way to put the dimensionally reduced metric into this ‘more appropriate’ form. The metrics with the negative dynamical exponent means that we are forced to put them in the wrong form with opposite boundary with respect to time. The KK monopole solution with null Melvin twist seems to be well defined. Thus it is reasonable to take this case seriously to investigate whether this makes sense, along with other systems with a negative dynamical exponent. Here we calculate a few physical properties associated with this KK metric, postponing more serious investigations to the future.

Entanglement entropy

The entanglement entropy of the metric can be computed using the prescription given in [11]. Using a strip geometry, the entanglement entropy of the metric (1.1) with $a = 1$, $b = 1$ and $\eta_j = 1$ can be computed as

$$l = \int_0^{r_t} dr \frac{(r/r_t)^\alpha}{\sqrt{1 - (r/r_t)^{2\alpha}}} = -\frac{i\pi}{2} r_t, \quad (\text{B.32})$$

and

$$\mathcal{A} = L^{d-1} L_\xi \int_\epsilon^{r_t} dr \frac{\beta^{-1/2} r^{-\alpha}}{\sqrt{1 - (r/r_t)^{2\alpha}}} = \beta^{-1/2} L^{d-1} L_\xi \left(-\frac{i\pi r_t^2}{4} + \mathcal{O}(\epsilon^3) \right), \quad (\text{B.33})$$

where $\alpha = -1$ for the KK monopole metric (B.29). The entanglement entropy for a strip in the general metric (3.2) (with $\eta_i = 1$) is

$$\mathcal{S} = \frac{(RM_{Pl})^6}{4} \left(i \frac{l^2}{\pi} \frac{L^4 L_\xi}{R_\theta^9} - \mathcal{O}(\epsilon^3) \right), \quad (\text{B.34})$$

where R_θ is a scale in which the hyperscaling violation becomes important. The result is rather unusual. The length l is imaginary and the entanglement entropy is also imaginary.

Holographic stress energy tensor

Let us calculate the stress energy tensor for this case.

$$\langle T_{tt} \rangle = -\frac{d+2-z-(d+1)\theta/D}{r_c^{d+2-(d+1)\theta/D}} h_{00} = -\frac{-1}{r_c^{-2}} h_{00}, \quad (\text{B.35})$$

$$\langle T_{t\xi} \rangle = \langle T_{\xi t} \rangle = -\frac{(d+1)(1-\theta/D)}{r_c^{d+2-(d+1)\theta/D}} h_{t\xi} = -\frac{-3}{r_c^{-2}} h_{t\xi}, \quad (\text{B.36})$$

$$\langle T_{ij} \rangle = -\frac{(d+1)(1-\theta/D)}{r_c^{d+2-(d+1)\theta/D}} h_{ij} = -\frac{-3}{r_c^{-2}} h_{ij}. \quad (\text{B.37})$$

The null energy condition is violated in this case. The stress energy tensor one point functions have opposite sign compared to the cases we consider above.

Semiclassical propagators

The static semiclassical propagator is given by

$$G(\Delta x_i) \sim \exp \left[2m \frac{D}{\theta} \epsilon^{\theta/D} \right] \exp \left[-m \frac{D}{\theta} c_{\theta/D} |\Delta x_i|^{\theta/D} \right],$$

$$c_{\theta/D} \equiv \left(\frac{2\sqrt{\pi} \Gamma \left(\frac{2-\theta/D}{2(1-\theta/D)} \right)}{\Gamma \left(\frac{1}{2(1-\theta/D)} \right)} \right)^{1-\theta/D}. \quad (\text{B.38})$$

where $\theta/D = 3/2$. The result is independent of z .

Outlook

Seemingly the physical properties show some unusual properties, such as imaginary entanglement entropy, stress energy tensors with wrong signs. Do they signal that this background is physically not acceptable? Instead of answering the question directly. We would like to bring out a system with negative dynamical exponent [12] along with the reference [124]. The latter discussed the Euclidean version of the metric similar to the one considered here (B.31). It will be interesting to investigate the systems with negative dynamical exponent along the line.

References

- [1] S. Sachdev, “*The Quantum phases of matter*,” 25th Solvay Conference on Physics, “The Theory of the Quantum World”, Brussels, Oct 2011, [arXiv:1203.4565][hep-th].
- [2] D. S. Fisher, “*Scaling and critical slowing down in random-field Ising systems*,” Phys. Rev. Lett. **56**, 416 (1986).
- [3] S. Sachdev, “*Quantum Phase Transitions*,” 2nd Ed., Cambridge University Press (2011).

- [4] C. Charmousis, B. Gouteraux, B. S. Kim, E. Kiritsis and R. Meyer, “*Effective Holographic Theories for low-temperature condensed matter systems*,” JHEP **1011**, 151 (2010) [[arXiv:1005.4690][hep-th].
- [5] B. Gouteraux and E. Kiritsis, “*Generalized Holographic Quantum Criticality at Finite Density*,” JHEP **1112**, 036 (2011) [arXiv:1107.2116][hep-th].
- [6] N. Ogawa, T. Takayanagi and T. Ugajin, “*Holographic Fermi Surfaces and Entanglement Entropy*,” [arXiv:1111.1023][hep-th].
- [7] L. Huijse, S. Sachdev and B. Swingle, “*Hidden Fermi surfaces in compressible states of gauge-gravity duality*,” [arXiv:1112.0573][cond-mat.str-el].
- [8] X. Dong, S. Harrison, S. Kachru, G. Torroba and H. Wang, “*Aspects of holography for theories with hyperscaling violation*,” [arXiv:1201.1905][hep-th].
- [9] E. Shaghoulian, “*Holographic Entanglement Entropy and Fermi Surfaces*,” [arXiv:1112.2702][hep-th].
- [10] K. Narayan, “*On Lifshitz scaling and hyperscaling violation in string theory*,” Phys. Rev. D **85**, 106006 (2012) [arXiv:1202.5935][hep-th].
- [11] B. S. Kim, “*Schrödinger Holography with and without Hyperscaling Violation*,” JHEP **1206**, 116 (2012) [arXiv:1202.6062][hep-th].
- [12] H. Singh, “*Lifshitz/Schrödinger Dp-branes and dynamical exponents*,” [arXiv:1202.6533][hep-th].
- [13] S. A. Hartnoll and E. Shaghoulian, “*Spectral weight in holographic scaling geometries*,” [arXiv:1203.4236][hep-th].
- [14] P. Dey and S. Roy, “*Lifshitz-like space-time from intersecting branes in string/M theory*,” [arXiv:1203.5381][hep-th].
- [15] Y. S. Myung and T. Moon, “*Quasinormal frequencies and thermodynamic quantities for the Lifshitz black holes*,” Phys. Rev. D **86**, 024006 (2012) [arXiv:1204.2116][hep-th].
- [16] P. Dey and S. Roy, “*Intersecting D-branes and Lifshitz-like space-time*,” [arXiv:1204.4858][hep-th].
- [17] E. Perlmutter, “*Hyperscaling violation from supergravity*,” JHEP **1206**, 165 (2012) [arXiv:1205.0242][hep-th].

- [18] M. Cadoni and S. Mignemi, “*Phase transition and hyperscaling violation for scalar Black Branes,*” JHEP **1206**, 056 (2012) [arXiv:1205.0412][hep-th].
- [19] C. Charmousis, B. Gouteraux and E. Kiritsis, “*Higher-derivative scalar-vector-tensor theories: black holes, Galileons, singularity cloaking and holography,*” [arXiv:1206.1499][hep-th].
- [20] M. Ammon, M. Kaminski and A. Karch, “*Hyperscaling-Violation on Probe D-Branes,*” [arXiv:1207.1726][hep-th].
- [21] E. Kiritsis, “*Lorentz violation, Gravity, Dissipation and Holography,*” [arXiv:1207.2325][hep-th].
- [22] J. Bhattacharya, S. Cremonini and A. Sinkovics, “*On the IR completion of geometries with hyperscaling violation,*” [arXiv:1208.1752][hep-th].
- [23] P. Dey and S. Roy, “*Holographic entanglement entropy of the near horizon 1/4 BPS F-Dp bound states,*” [arXiv:1208.1820][hep-th].
- [24] N. Kundu, P. Narayan, N. Sircar and S. P. Trivedi, “*Entangled Dilaton Dyons,*” [arXiv:1208.2008][hep-th].
- [25] M. Kulaxizi, A. Parnachev and K. Schalm, “*On Holographic Entanglement Entropy of Charged Matter,*” [arXiv:1208.2937][hep-th].
- [26] M. Alishahiha and H. Yavartanoo, “*On Holography with Hyperscaling Violation,*” [arXiv:1208.6197][hep-th].
- [27] C. Park, “*Membrane paradigm in the Einstein-dilaton theory,*” [arXiv:1209.0842][hep-th].
- [28] P. Dey and S. Roy, “*Lifshitz metric with hyperscaling violation from NS5-Dp states in string theory,*” [arXiv:1209.1049][hep-th].
- [29] J. Sadeghi, B. Pourhassan and A. Asadi, “*Thermodynamics of string black hole with hyperscaling violation,*” [arXiv:1209.1235][hep-th].
- [30] J. Sadeghi, B. Pourhasan and F. Poursadollah, “*Schrödinger black holes with hyperscaling violation,*” [arXiv:1209.1874][hep-th].
- [31] S. S. Pal, “*Fermi-like Liquid From Einstein-DBI-Dilaton System,*” [arXiv:1209.3559][hep-th].

- [32] M. Alishahiha, E. OColgain and H. Yavartanoo, “*Charged Black Branes with Hyperscaling Violating Factor*,” [arXiv:1209.3946][hep-th].
- [33] P. Bueno, W. Chemissany, P. Meessen, T. Ortin and C. S. Shahbazi, “*Lifshitz-like solutions with hyperscaling violation in ungauged supergravity*,” [arXiv:1209.4047][hep-th].
- [34] K. Narayan, “*AdS null deformations with inhomogeneities*,” [arXiv:1209.4348][hep-th].
- [35] M. Cadoni and M. Serra, “*Hyperscaling violation for scalar black branes in arbitrary dimensions*,” [arXiv:1209.4484][hep-th].
- [36] J. M. Maldacena, “*The Large N limit of superconformal field theories and supergravity*,” Adv. Theor. Math. Phys. **2**, 231 (1998) [arXiv:hep-th/9711200].
- [37] O. Aharony, S. S. Gubser, J. M. Maldacena, H. Ooguri and Y. Oz, “*Large N field theories, string theory and gravity*,” Phys. Rept. **323**, 183 (2000) [arXiv:hep-th/9905111].
- [38] L. Huijse and S. Sachdev, “*Fermi surfaces and gauge-gravity duality*,” Phys. Rev. D **84**, 026001 (2011) [arXiv:1104.5022][hep-th].
- [39] S. Sachdev, “*Compressible quantum phases from conformal field theories in 2+1 dimensions*,” [arXiv:1209.1637][hep-th].
- [40] S. -S. Lee, “*A Non-Fermi Liquid from a Charged Black Hole: A Critical Fermi Ball*,” Phys. Rev. D **79**, 086006 (2009) [arXiv:0809.3402][hep-th].
- [41] H. Liu, J. McGreevy and D. Vegh, “*Non-Fermi liquids from holography*,” Phys. Rev. D **83**, 065029 (2011) [arXiv:0903.2477][hep-th].
- [42] M. Cubrovic, J. Zaanen and K. Schalm, “*String Theory, Quantum Phase Transitions and the Emergent Fermi-Liquid*,” Science **325**, 439 (2009) [arXiv:0904.1993][hep-th].
- [43] T. Faulkner, H. Liu, J. McGreevy and D. Vegh, “*Emergent quantum criticality, Fermi surfaces, and AdS(2)*,” Phys. Rev. D **83**, 125002 (2011) [arXiv:0907.2694][hep-th].
- [44] N. Doiron-Leyraud et. al., “*Quantum oscillations and the Fermi surface in an underdoped high- T_c superconductor*,” Nature 447, 565 (2007).
- [45] J. Eisert, M. Cramer and M. B. Plenio, “*Area laws for the entanglement entropy - a review*,” Rev. Mod. Phys. **82**, 277 (2010) [arXiv:0808.3773][quant-ph].

- [46] S. Ryu and T. Takayanagi, “*Holographic derivation of entanglement entropy from AdS/CFT*,” Phys. Rev. Lett. **96** (2006) 181602 [arXiv:hep-th/0603001].
- [47] S. Ryu and T. Takayanagi, “*Aspects of holographic entanglement entropy*,” JHEP **0608** (2006) 045 [arXiv:hep-th/0605073].
- [48] V. E. Hubeny, M. Rangamani and T. Takayanagi, “*A Covariant holographic entanglement entropy proposal*,” JHEP **0707**, 062 (2007) [arXiv:0705.0016][hep-th].
- [49] T. Takayanagi, “*Entanglement Entropy from a Holographic Viewpoint*,” Class. Quant. Grav. **29**, 153001 (2012) [arXiv:1204.2450][gr-qc].
- [50] K. Balasubramanian and J. McGreevy, “*An Analytic Lifshitz black hole*,” Phys. Rev. D **80**, 104039 (2009) [arXiv:0909.0263][hep-th].
- [51] B. Gouteraux, B. S. Kim and R. Meyer, “*Charged Dilatonic Black Holes and their Transport Properties*,” Fortsch. Phys. **59**, 723 (2011) [arXiv:1102.4440][hep-th].
- [52] R. Meyer, B. Gouteraux and B. S. Kim, “*Strange Metallic Behaviour and the Thermodynamics of Charged Dilatonic Black Holes*,” Fortsch. Phys. **59**, 741 (2011) [arXiv:1102.4433][hep-th].
- [53] A. Hashimoto and N. Itzhaki, “*Noncommutative Yang-Mills and the AdS / CFT correspondence*,” Phys. Lett. B **465**, 142 (1999) [hep-th/9907166].
- [54] J. M. Maldacena and J. G. Russo, “*Large N limit of noncommutative gauge theories*,” JHEP **9909**, 025 (1999) [hep-th/9908134].
- [55] M. Alishahiha, Y. Oz and J. G. Russo, “*Supergravity and light - like noncommutativity*,” JHEP **0009**, 002 (2000) [arXiv:hep-th/0007215].
- [56] V. E. Hubeny, M. Rangamani and S. F. Ross, “*Causal structures and holography*,” JHEP **0507**, 037 (2005) [arXiv:hep-th/0504034].
- [57] A. Bergman, K. Dasgupta, O. J. Ganor, J. L. Karczmarek and G. Rajesh, “*Nonlocal field theories and their gravity duals*,” Phys. Rev. D **65**, 066005 (2002) [arXiv:hep-th/0103090].
- [58] A. Bergman and O. J. Ganor, “*Dipoles, twists and noncommutative gauge theory*,” JHEP **0010**, 018 (2000) [arXiv:hep-th/0008030].
- [59] O. J. Ganor, “*A New Lorentz violating nonlocal field theory from string-theory*,” Phys. Rev. D **75**, 025002 (2007) [arXiv:hep-th/0609107].

- [60] O. J. Ganor, A. Hashimoto, S. Jue, B. S. Kim and A. Ndirango, “*Aspects of Puff Field Theory*,” JHEP **0708**, 035 (2007) [arXiv:hep-th/0702030].
- [61] S. Kachru, X. Liu and M. Mulligan, “*Gravity Duals of Lifshitz-like Fixed Points*,” Phys. Rev. D **78**, 106005 (2008) [arXiv:0808.1725][hep-th].
- [62] M. Taylor, “*Non-relativistic holography*,” [arXiv:0812.0530][hep-th].
- [63] C. Charmousis, B. Gouteraux and J. Soda, “*Einstein-Maxwell-Dilaton theories with a Liouville potential*,” Phys. Rev. D **80**, 024028 (2009) [arXiv:0905.3337][gr-qc].
- [64] S. S. Gubser and F. D. Rocha, “*Peculiar properties of a charged dilatonic black hole in AdS_5* ,” Phys. Rev. D **81**, 046001 (2010) [arXiv:0911.2898][hep-th].
- [65] K. Goldstein, S. Kachru, S. Prakash and S. P. Trivedi, “*Holography of Charged Dilaton Black Holes*,” JHEP **1008**, 078 (2010) [arXiv:0911.3586][hep-th].
- [66] M. Cadoni, G. D’Appollonio and P. Pani, “*Phase transitions between Reissner-Nordstrom and dilatonic black holes in 4D AdS spacetime*,” JHEP **1003**, 100 (2010) [arXiv:0912.3520][hep-th].
- [67] M. Cadoni and P. Pani, “*Holography of charged dilatonic black branes at finite temperature*,” JHEP **1104**, 049 (2011) [arXiv:1102.3820][hep-th].
- [68] G. Bertoldi, B. A. Burrington and A. W. Peet, “*Thermal behavior of charged dilatonic black branes in AdS and UV completions of Lifshitz-like geometries*,” Phys. Rev. D **82**, 106013 (2010) [arXiv:1007.1464][hep-th].
- [69] G. Bertoldi, B. A. Burrington, A. W. Peet and I. G. Zadeh, “*Lifshitz-like black brane thermodynamics in higher dimensions*,” Phys. Rev. D **83**, 126006 (2011) [arXiv:1101.1980][hep-th].
- [70] K. Goldstein, N. Iizuka, S. Kachru, S. Prakash, S. P. Trivedi and A. Westphal, “*Holography of Dyonically Charged Dilaton Black Branes*,” JHEP **1010**, 027 (2010) [arXiv:1007.2490][hep-th].
- [71] N. Iizuka, N. Kundu, P. Narayan and S. P. Trivedi, “*Holographic Fermi and Non-Fermi Liquids with Transitions in Dilaton Gravity*,” [arXiv:1105.1162][hep-th].
- [72] B. -H. Lee, D. -W. Pang and C. Park, “*Strange Metallic Behavior in Anisotropic Background*,” JHEP **1007**, 057 (2010) [arXiv:1006.1719][hep-th].
- [73] P. Berglund, J. Bhattacharyya and D. Mattingly, “*Charged Dilatonic AdS Black Branes in Arbitrary Dimensions*,” [arXiv:1107.3096][hep-th].

- [74] B. Gouteraux, J. Smolic, M. Smolic, K. Skenderis and M. Taylor, “*Holography for Einstein-Maxwell-dilaton theories from generalized dimensional reduction*,” JHEP **1201**, 089 (2012) [arXiv:1110.2320][hep-th].
- [75] S. S. Gubser, “*Curvature singularities: The Good, the bad, and the naked*,” Adv. Theor. Math. Phys. **4**, 679 (2000) [hep-th/0002160].
- [76] C. Hoyos and P. Koroteev, “*On the Null Energy Condition and Causality in Lifshitz Holography*,” Phys. Rev. D **82**, 084002 (2010) [Erratum-ibid. D **82**, 109905 (2010)] [arXiv:1007.1428][hep-th].
- [77] B. Swingle and T. Senthil, “*Universal crossovers between entanglement entropy and thermal entropy*,” [arXiv:1112.1069][cond-mat.str-el].
- [78] U. Gursoy, E. Kiritsis and F. Nitti, “*Exploring improved holographic theories for QCD: Part II*,” JHEP **0802**, 019 (2008) [arXiv:0707.1349][hep-th].
- [79] U. Gursoy, E. Kiritsis, L. Mazzanti and F. Nitti, “*Holography and Thermodynamics of 5D Dilaton-gravity*,” JHEP **0905**, 033 (2009) [arXiv:0812.0792][hep-th].
- [80] C. Charmousis, R. Emparan and R. Gregory, “*Selfgravity of brane worlds: A New hierarchy twist*,” JHEP **0105**, 026 (2001) [hep-th/0101198].
- [81] D. T. Son, “*Toward an AdS/cold atoms correspondence: a geometric realization of the Schroedinger symmetry*,” Phys. Rev. D **78**, 046003 (2008) [arXiv:0804.3972][hep-th].
- [82] K. Balasubramanian and J. McGreevy, “*Gravity duals for non-relativistic CFTs*,” Phys. Rev. Lett. **101**, 061601 (2008) [arXiv:0804.4053][hep-th].
- [83] C. P. Herzog, M. Rangamani and S. F. Ross, “*Heating up Galilean holography*,” JHEP **0811**, 080 (2008) [arXiv:0807.1099][hep-th].
- [84] J. Maldacena, D. Martelli and Y. Tachikawa, “*Comments on string theory backgrounds with non-relativistic conformal symmetry*,” JHEP **0810**, 072 (2008) [arXiv:0807.1100][hep-th].
- [85] A. Adams, K. Balasubramanian and J. McGreevy, “*Hot Spacetimes for Cold Atoms*,” JHEP **0811**, 059 (2008) [arXiv:0807.1111][hep-th].
- [86] D. Yamada, “*Thermodynamics of Black Holes in Schroedinger Space*,” Class. Quant. Grav. **26**, 075006 (2009) [arXiv:0809.4928][hep-th].
- [87] M. Ammon, C. Hoyos, A. O’Bannon and J. M. S. Wu, “*Holographic Flavor Transport in Schrodinger Spacetime*,” JHEP **1006**, 012 (2010) [arXiv:1003.5913][hep-th].

- [88] M. Alishahiha and O. J. Ganor, “*Twisted backgrounds, PP waves and nonlocal field theories,*” JHEP **0303**, 006 (2003) [arXiv:hep-th/0301080].
- [89] E. G. Gimon, A. Hashimoto, V. E. Hubeny, O. Lunin and M. Rangamani, “*Black strings in asymptotically plane wave geometries,*” JHEP **0308**, 035 (2003) [arXiv:hep-th/0306131].
- [90] L. Mazzucato, Y. Oz and S. Theisen, “*Non-relativistic Branes,*” JHEP **0904**, 073 (2009) [arXiv:0810.3673][hep-th].
- [91] C. Duval, M. Hassaine and P. A. Horvathy, “*The Geometry of Schrodinger symmetry in gravity background/non-relativistic CFT,*” Annals Phys. **324**, 1158 (2009) [arXiv:0809.3128][hep-th].
- [92] S. A. Hartnoll and K. Yoshida, “*Families of IIB duals for nonrelativistic CFTs,*” JHEP **0812**, 071 (2008) [arXiv:0810.0298][hep-th].
- [93] A. Adams, A. Maloney, A. Sinha and S. E. Vazquez, “*1/N Effects in Non-Relativistic Gauge-Gravity Duality,*” JHEP **0903**, 097 (2009) [arXiv:0812.0166][hep-th].
- [94] J. P. Gauntlett, S. Kim, O. Varela and D. Waldram, “*Consistent supersymmetric Kaluza-Klein truncations with massive modes,*” JHEP **0904**, 102 (2009) [arXiv:0901.0676][hep-th].
- [95] A. Donos and J. P. Gauntlett, “*Supersymmetric solutions for non-relativistic holography,*” JHEP **0903**, 138 (2009) [arXiv:0901.0818][hep-th].
- [96] S. S. Pal, “*Non-relativistic supersymmetric Dp branes,*” Class. Quant. Grav. **26**, 245014 (2009) [arXiv:0904.3620][hep-th].
- [97] N. Bobev, A. Kundu and K. Pilch, “*Supersymmetric IIB Solutions with Schrodinger Symmetry,*” JHEP **0907**, 107 (2009) [arXiv:0905.0673][hep-th].
- [98] A. Donos and J. P. Gauntlett, “*Solutions of type IIB and D=11 supergravity with Schrodinger(z) symmetry,*” JHEP **0907**, 042 (2009) [arXiv:0905.1098][hep-th].
- [99] E. O. Colgain, O. Varela and H. Yavartanoo, “*Non-relativistic M-Theory solutions based on Kaehler-Einstein spaces,*” JHEP **0907**, 081(2009) [arXiv:0906.0261][hep-th].
- [100] S. Cremonesi, D. Melnikov and Y. Oz, “*Stability of Asymptotically Schrödinger RN Black Hole and Superconductivity,*” JHEP **1004**, 048 (2010) [arXiv:0911.3806][hep-th].

- [101] J. Jeong, H. C. Kim, S. Lee, E. O Colgain and H. Yavartanoo, “*Schrodinger invariant solutions of M-theory with Enhanced Supersymmetry*,” JHEP **1003**, 034 (2010) [arXiv:0911.5281][hep-th].
- [102] N. Banerjee, S. Dutta and D. P. Jatkar, “*Geometry and Phase Structure of Non-Relativistic Branes*,” Class. Quant. Grav.**28**,165002 (2011) [arXiv:1102.0298][hep-th].
- [103] P. Kraus and E. Perlmutter, “*Universality and exactness of Schrodinger geometries in string and M-theory*,” JHEP **1105**, 045 (2011) [arXiv:1102.1727][hep-th].
- [104] H. -C. Kim, S. Kim, K. Lee and J. Park, “*Emergent Schrodinger geometries from mass-deformed CFT*,” JHEP **1108**, 111 (2011) [arXiv:1106.4309][hep-th].
- [105] C. M. Brown and O. DeWolfe, “*The Godel-Schrodinger Spacetime and Stringy Chronology Protection*,” JHEP **1201**, 032 (2012) [arXiv:1110.3840][hep-th].
- [106] S. Hyun, J. Jeong and B. S. Kim, “*Finite Temperature Aging Holography*,” JHEP **1203**, 010 (2012) [arXiv:1108.5549][hep-th].
- [107] S. Hyun, J. Jeong and B. S. Kim, “*Aging Logarithmic Conformal Field Theory : a holographic view*,” [arXiv:1209.2417][hep-th].
- [108] M. Guica, K. Skenderis, M. Taylor and B. C. van Rees, “*Holography for Schrodinger backgrounds*,” JHEP **1102**, 056 (2011) [arXiv:1008.1991][hep-th].
- [109] K. Balasubramanian and J. McGreevy, “*The Particle number in Galilean holography*,” JHEP **1101**, 137 (2011) [arXiv:1007.2184][hep-th].
- [110] N. Itzhaki, J. M. Maldacena, J. Sonnenschein, and S. Yankielowicz, “*Supergravity and the large N limit of theories with sixteen supercharges*,” Phys. Rev. **D58** (1998) 046004, [hep-th/9802042].
- [111] H. Boonstra, K. Skenderis, and P. Townsend, “*The domain wall / QFT correspondence*,” JHEP **9901** (1999) 003, [hep-th/9807137].
- [112] B. S. Kim and D. Yamada, “*Properties of Schroedinger Black Holes from AdS Space*,” JHEP **1107**, 120 (2011) [arXiv:1008.3286][hep-th].
- [113] N. Bobev and B. C. van Rees, “*Schrodinger Deformations of AdS₃xS³*,” JHEP **1108**, 062 (2011) [arXiv:1102.2877][hep-th].
- [114] R. N. Caldeira Costa and M. Taylor, “*Holography for chiral scale-invariant models*,” JHEP **1102**, 082 (2011) [arXiv:1010.4800][hep-th].

- [115] W. D. Goldberger, “*AdS/CFT duality for non-relativistic field theory*,” JHEP **0903**, 069 (2009) [arXiv:0806.2867][hep-th].
- [116] J. L. F. Barbon and C. A. Fuertes, “*On the spectrum of nonrelativistic AdS/CFT*,” JHEP **0809**, 030 (2008) [arXiv:0806.3244][hep-th].
- [117] B. S. Kim, E. Kiritsis and C. Panagopoulos, “*Holographic quantum criticality and strange metal transport*,” New J. Phys. **14**, 043045 (2012) [arXiv:1012.3464][cond-mat.str-el].
- [118] K. -Y. Kim and D. -W. Pang, “*Holographic DC conductivities from the open string metric*,” JHEP **1109**, 051 (2011) [arXiv:1108.3791][hep-th].
- [119] K. B. Fadafan, “*Strange metals at finite 't Hooft coupling*,” [arXiv:1208.1855][hep-th].
- [120] G. T. Horowitz, J. M. Maldacena and A. Strominger, “*Nonextremal black hole microstates and U duality*,” Phys. Lett. B **383**, 151 (1996) [arXiv:hep-th/9603109].
- [121] A. A. Tseytlin, “*Composite BPS configurations of p-branes in ten-dimensions and eleven-dimensions*,” Class. Quant. Grav. **14**, 2085 (1997) [arXiv:hep-th/9702163].
- [122] J. M. Maldacena and H. Ooguri, “*Strings in AdS(3) and the SL(2,R) WZW model. Part 3. Correlation functions*,” Phys. Rev. D **65**, 106006 (2002) [arXiv:hep-th/0111180].
- [123] H. J. Boonstra, B. Peeters and K. Skenderis, “*Duality and asymptotic geometries*,” Phys. Lett. B **411**, 59 (1997) [arXiv:hep-th/9706192].
- [124] M. Cvetič, H. Lu and C. N. Pope, “*Space-times of boosted p-branes and CFT in infinite momentum frame*,” Nucl. Phys. B **545**, 309 (1999) [arXiv:hep-th/9810123].